

TTP04-01
 SFB/CPP-04-43
 hep-ph/0401087

Next-to-leading mass singularities in two-loop electroweak singlet form factors

S. POZZORINI[†]

*Institut für Theoretische Teilchenphysik, Universität Karlsruhe
 D-76128 Karlsruhe, Germany*

Abstract:

We consider virtual electroweak corrections to the form factors for massless chiral fermions coupling to an $SU(2) \times U(1)$ singlet gauge boson in the asymptotic region $s \gg M_W^2 \sim M_Z^2$, where the invariant mass s of the external gauge boson is much higher than the weak-boson mass scale. Using the sector-decomposition method we compute mass singularities, which arise as logarithms of s/M_W^2 and $1/\epsilon$ poles in $D = 4 - 2\epsilon$ dimensions, to one- and two-loop next-to-leading-logarithmic accuracy. In this approximation we include all contributions of order $\alpha^l \epsilon^k \log^{j+k}(s/M_W^2)$, with $l = 1, 2$ and $j = 2l, 2l - 1$. We find that the electroweak two-loop leading- and next-to-leading-logarithmic mass singularities can be written in a form that corresponds to a generalization of Catani's formula for massless QCD.

January 2004

[†]pozzorin@particle.uni-karlsruhe.de

1 Introduction

Future colliders, such as the LHC [1] or an e^+e^- Linear Collider (LC) [2, 3, 4], will investigate interactions between the constituents of the Standard Model in a new window of energies above the present frontier of few hundred GeV up to the TeV scale and with very high luminosities. On the one hand, this window will provide new insights into the mechanism of electroweak (EW) symmetry-breaking through either the discovery of the Higgs boson and the measurement of its couplings or the observation of strongly interacting vector bosons. On the other hand, it will open new perspectives for precision tests of the Standard Model.

From the point of view of theoretical predictions, since the size of radiative corrections grows with energy, multi-loop calculations will play an increasingly important role, especially in order to achieve the permille-level accuracy required by a machine such as a LC. In this context, the behaviour of the EW corrections is particularly interesting. Indeed, if one considers the range of energies much higher than the weak-boson mass scale, $\sqrt{s} \gg M_W$, and performs an expansion in M_W/\sqrt{s} , the leading terms of this expansion arise as a tower of logarithms [5],

$$\alpha^l \log^j \left(\frac{s}{M_W^2} \right), \quad \text{with} \quad 0 \leq j \leq 2l, \quad (1.1)$$

which clearly enhance the EW corrections. At $\sqrt{s} = 1$ TeV, these logarithms yield one-loop EW corrections of tens of percent with a considerable impact on LHC observables, and two-loop corrections of a few percent, which must be under control at a LC.

At l -loop level, the leading logarithms (LL's), also known as Sudakov logarithms [6], have power $j = 2l$, and the subleading terms with $j = 2l-1, 2l-2, \dots$ are denoted as next-to-leading logarithms (NLL's), next-to-next-to-leading logarithms (NNLL's), and so on. Analogously to mass singularities observed in QED and QCD, the EW logarithms arise from soft/collinear emission of virtual or real particles off initial or final-state particles. However, in contrast to QED and QCD, the EW logarithms do not cancel in physical observables since the weak-boson masses provide a physical cut-off and there is no need to include real Z- and W-boson bremsstrahlung. Moreover, even observables that are fully inclusive with respect to Z- and W-bremsstrahlung are affected by EW LL's that violate the Bloch–Nordsieck theorem [7], owing to the fact that the scattering particles (fermions or gauge bosons) carry non-abelian weak-isospin charges.

At one loop, the EW LL's and NLL's are now well understood. On the one hand, explicit diagrammatic calculations for many $2 \rightarrow 2$ processes exist [8, 9, 10, 11]. On the other hand, it has been proven that these logarithms are universal, and general results have been given for arbitrary processes that are not mass-suppressed at high energies [12, 13]. For gauge-boson pair production at the LHC it was shown that, in the transverse-momentum region above few-hundred GeV, the EW logarithmic corrections can become of the order of the QCD corrections [14].

At two loops, the situation is more difficult, since the analytical evaluation of Feynman diagrams with many external legs and different internal masses is a highly non-trivial task. At present, there are good prospects to compute vertex diagrams that depend on one single dimensionless parameter M_W^2/s [15]. However, exact analytical results for general $2 \rightarrow 2$

processes seem to be out of reach. It is therefore reasonable either to solve the problem numerically, as for instance in Ref. [16], or to use analytical approximations.

Two different strategies have been adopted in order to treat the higher-order EW logarithms analytically. On the one hand, evolution equations, which are well known in QED and QCD, have been applied to the EW theory in order to resum the one-loop logarithms¹. On the other hand, explicit diagrammatic calculations have been performed using, for instance, the Sudakov method or the eikonal approximation.

Fadin *et al.* [17] have resummed the EW leading-logarithmic (LL) corrections to arbitrary matrix elements by means of the infrared evolution equation (IREE). Kühn *et al.* have resummed the EW logarithmic corrections to massless 4-fermion processes up to the NNLL's [18]. At the TeV scale they found that, for these particular processes, the leading and subleading logarithms have similar size and alternating signs, which gives rise to large cancellations. This means that, depending on the process, it might be necessary to compute the complete tower of logarithms (1.1). A prescription for the resummation of the next-to-leading-logarithmic (NLL) corrections to arbitrary processes has been proposed by Melles [19, 20].

All the above resummations are based on the idea of splitting the EW theory into two regimes, both with exact gauge symmetry. This idea was first formulated in the context of the IREE [17], which describes the all-order LL dependence of matrix elements with respect to the transverse-momentum cut-off μ_\perp within symmetric gauge theories. In practice, for the regime $\sqrt{s} \geq \mu_\perp \geq M_W$ all EW gauge bosons are supposed to behave as if they would have the same mass M_W and one assumes $SU(2) \times U(1)$ symmetry, whereas in the regime $M_W \geq \mu_\perp$ the weak bosons are supposed to be frozen out and $U(1)_{\text{em}}$ symmetry is assumed. This latter regime describes the effects originating from the mass gap in the gauge sector, i.e. from the fact that the (massless) photon is much lighter than the weak bosons.

We note that in the above resummations, apart from the splitting of the evolution into two regimes, no other effects from spontaneous symmetry breaking are considered. In particular, the following assumptions are explicitly or implicitly made.

- (i) In the massless limit $M_W^2/s \rightarrow 0$, all couplings with mass dimension, which originate from symmetry breaking, are neglected.
- (ii) The weak-boson masses are introduced in the corresponding propagators as regulators of soft and collinear singularities from W and Z bosons without spontaneous symmetry breaking. Since these masses are of the same order, one considers $M_W = M_Z$.
- (iii) The regimes above and below the EW scale are treated as an unmixed $SU(2) \times U(1)$ theory and QED, respectively, and mixing effects in the gauge sector are neglected.

It is important to understand to which extend the above assumptions are legitimate and whether the resulting resummation prescriptions are correct. This can be done by explicit

¹In order to resum the LL's and NLL's it is sufficient to determine the kernel of the evolution equations to one-loop accuracy. However, starting from the NNLL's also the two-loop contributions to the β -function and to the anomalous dimensions are needed.

diagrammatic two-loop calculations based on the EW Lagrangian, where all effects related to spontaneous symmetry breaking are consistently taken into account.

At the LL level, these checks have been already completed. A calculation of the massless fermionic singlet form factor [21, 22] and then a Coulomb-gauge calculation for arbitrary processes [23] have demonstrated that the EW LL's exponentiate as predicted by the IREE. Also the angular-dependent subset of the NLL's has been shown to exponentiate for arbitrary processes [24] as anticipated in Refs. [18, 20]. The complete tower of two-loop logarithms has been computed in Ref. [25] for the fermionic and scalar subsets of the corrections to a massless fermionic form factor within an abelian massive theory.

In this paper we present a first diagrammatic calculation where the complete set of EW LL and NLL corrections is taken into account. We consider the one- and two-loop virtual EW corrections to the form factors for massless chiral fermions coupling to an $SU(2) \times U(1)$ singlet gauge boson. All relevant loop integrals within the 't Hooft–Feynman gauge are evaluated in the asymptotic region $s \gg M_W^2 \sim M_Z^2$ to NLL accuracy using the sector-decomposition method. In addition to the logarithms of the type (1.1), which arise from massive virtual particles, we include also mass singularities from massless photons. These latter are regulated dimensionally and arise as $1/\epsilon$ poles in $D = 4 - 2\epsilon$ dimensions. In NLL approximation all mass singularities of the order $\alpha^l \epsilon^k \log^{j+k}(s/M_W^2)$, with $j = 2l, 2l - 1$, and $-j \leq k \leq 4 - 2l$, are taken into account. We do not assume $M_Z = M_W$ and we include contributions depending on $\log(M_Z/M_W)$.

The paper is organized as follows. In Sect. 2 we define our conventions for the chiral form factors and for the computation of the logarithmic EW corrections. The one-loop results are presented in Sect. 3. In Sect. 4 we provide the two-loop contributions from individual Feynman diagrams and counterterms and present the final result. A detailed discussion is given in Sect. 5. The definitions of the relevant one- and two-loop integrals as well as group-theoretical quantities related to the β -function can be found in the appendices.

2 Definitions and conventions

In this section we introduce chiral form factors and corresponding projectors for the vertex involving an external $SU(2) \times U(1)$ singlet gauge boson and a massless fermion–antifermion pair. We define the conventions used to calculate the EW corrections, the NLL approximation, and a subtraction to isolate mass-gap effects.

2.1 Chiral form factors in D dimensions

Let us consider the vertex function

$$= i\bar{u}(p_1) F^\nu v(p_2) \quad (2.1)$$

with a fermion–antifermion pair coupled to an external gauge boson. This latter, which might be for instance a gluon, is treated as an external field that does not enter the virtual corrections. Moreover, it is assumed to be an $SU(2) \times U(1)$ singlet, which does not interact with the EW gauge bosons but only with fermions.

The outgoing fermionic momenta and the invariant mass of the gauge boson are denoted as p_1, p_2 , and $s = (p_1 + p_2)^2$, respectively. We assume that the fermions are on-shell and massless. In this case, the above vertex can be parametrized in terms of the left- and right-handed form factors F_- and F_+ as

$$F^\nu = \gamma^\nu \sum_{\sigma=\pm} \omega_\sigma F_\sigma, \quad \text{with} \quad \omega_\pm = \frac{1}{2}(1 \pm \gamma^5), \quad (2.2)$$

where indices corresponding to the weak isospin of the external fermions are implicitly understood. The couplings of the singlet gauge boson to the fermions are given by the tree-level form factors and can be in general parity violating.

Since we compute the loop corrections within dimensional regularization, we have to specify a prescription to handle γ^5 in $D = 4 - 2\epsilon$ dimensions without violating the Ward identities of the external current. In principle, a chiral anomaly could originate from fermionic triangle subdiagrams. However, such triangle subdiagrams, and the corresponding chiral anomaly, do not contribute to the leading and next-to-leading mass singularities (see Sect. 2.3) that we calculate in this paper. Therefore, we can safely adopt a dimensional regularization scheme with

$$\{\gamma^\mu, \gamma^5\} = 0. \quad (2.3)$$

We note that this choice of scheme is not unique. In principle, other prescriptions could be used which differ with respect to (2.3) by terms of order ϵ . As a consequence, the residues of the subleading $1/\epsilon$ poles in the infrared-divergent virtual and real corrections are scheme dependent. However, this ambiguity disappears in their infrared-finite combination, provided that the same prescription (2.3) is used for virtual and real corrections.

2.2 Chiral projectors

The left- and right-handed form factors F_{\pm} can be obtained by means of the following projectors

$$F_{\sigma} = \mathcal{P}_{\sigma} \left(\text{Diagram: a wavy line with a loop, followed by a shaded circle with two outgoing lines} \right) := \frac{1}{(2-D)s} \text{Tr} (\gamma_{\nu} \not{p}_1 F^{\nu} \omega_{\sigma} \not{p}_2). \quad (2.4)$$

When these projections \mathcal{P}_{σ} are applied to loop diagrams, the chiral projectors ω_{σ} can be easily combined with those originating from the couplings of the massless fermions to virtual EW gauge bosons $V = A, Z, W^{\pm}$,

$$\text{Diagram: a wavy line } V_{\mu} \text{ meets a fermion line } \bar{\Psi}_i \text{ and a fermion line } \Psi_j \text{ at a vertex.} = ie\gamma_{\mu} \sum_{\rho=\pm} \omega_{\rho} (I_{\rho}^V)_{\Psi_i \Psi_j}. \quad (2.5)$$

Here $\Psi_i = u, d$ are the components of the fermionic doublet Ψ , and the generators I_{ρ}^V [see (2.24)] are isospin matrices in the representation corresponding to the chirality ρ , i.e. the fundamental or singlet representation for left-handed ($\rho = -$) or right-handed ($\rho = +$) chirality, respectively.

In practice, as a result of chirality conservation for massless fermions, in each vertex (2.5) that is connected to the external gauge boson by means of a massless fermionic line one can replace $\sum_{\rho} \omega_{\rho} I_{\rho}^V$ by I_{σ}^V , i.e. the right- and left-handed form factors (2.4) receive contributions only from couplings with corresponding chirality $\rho = \sigma$. After this simplification, owing to the fact that the form factors depend only on two linearly independent external momenta, which cannot give rise to a totally antisymmetric tensor with four indices, the remaining γ^5 contribution from ω_{σ} drops out and one can set $\omega_{\sigma} = 1/2$ in (2.4).

2.3 Perturbative and asymptotic expansions

As a convention, we write the perturbative expansion of the chiral form factors as

$$F_{\sigma} = F_{\sigma}^{(0)} \left[1 + \sum_{l=1}^{\infty} \left(\frac{\alpha}{4\pi} \right)^l N_{\epsilon}^l \delta F_{\sigma}^{(l)} \right] \quad \text{with} \quad N_{\epsilon} = \frac{1}{\Gamma(D/2 - 1)} \left(\frac{4\pi\mu_0^2}{-s} \right)^{2-D/2}, \quad (2.6)$$

where $\alpha = e^2/(4\pi)$ is the electromagnetic fine-structure constant, $\delta F_{\sigma}^{(l)}$ represent the l -loop corrections relative to the tree-level form factors $F_{\sigma}^{(0)}$, and the normalization factor N_{ϵ} , with μ_0 being the scale of dimensional regularization, is introduced in order to facilitate the

comparison with Ref. [26]. In the calculation, the l -loop contributions $\delta F_\sigma^{(l)}$ are extracted from the corresponding vertex functions $F_{(l)}^\nu$ by means of the normalized projectors

$$\bar{\mathcal{P}}_\sigma^{(l)} = \frac{(4\pi)^{2l}}{N_\epsilon^l} \mathcal{P}_\sigma, \quad \bar{\mathcal{P}}_\sigma^{(l)} [F_{(l)}^\nu] = e^{2l} F_\sigma^{(0)} \delta F_\sigma^{(l)}. \quad (2.7)$$

The EW corrections depend on the invariant mass s , on the masses of the heavy virtual particles W, Z, t , and H , as well as on the renormalization scales μ_i . In this paper we consider the asymptotic region

$$s \gg M_W^2 \sim M_Z^2 \sim m_t^2 \sim M_H^2, \quad (2.8)$$

where the invariant mass s is much higher than the EW scale. In order to simplify the discussion, let us assume for the moment that

$$M_W = M_Z = m_t = M_H, \quad (2.9)$$

and $\mu_i = M_W$. In this case, the EW corrections depend only on the dimensionless ratio s/M_W^2 , and are dominated by mass-singular logarithms²

$$L := \log \left(\frac{-s}{M_W^2} \right), \quad (2.10)$$

which originate from soft and collinear heavy particles. In addition we have mass singularities that originate from soft and collinear massless photons and give rise to $1/\epsilon$ poles in $D = 4 - 2\epsilon$ dimensions. Therefore, the l -loop contributions to the chiral form factors can be written as a double expansion in L and ϵ ,

$$\delta F_\sigma^{(l)} = \sum_{j=0}^{2l} \sum_{k=-j}^{\infty} \delta F_{\sigma;j,k}^{(l)} \epsilon^k L^{j+k}, \quad (2.11)$$

with coefficients $\delta F_{\sigma;j,k}^{(l)}$ that tend to constants in the asymptotic limit $s/M_W^2 \rightarrow \infty$.

In order to classify mass singularities, we define the degree of singularity of a term in (2.11) as the total power j of logarithms L and $1/\epsilon$ poles. The maximal degree of singularity at l -loop level is $j = 2l$ and the corresponding terms are denoted as LL's. The terms with $j = 2l - 1$ represent the NLL's, and so on.

In this paper we systematically neglect mass-suppressed corrections of order M_W^2/s and we calculate the one- and two-loop corrections to NLL accuracy, i.e. including LL's and NLL's. For this approximation we use the symbol $\stackrel{\text{NLL}}{=}$. The two-loop corrections are expanded in ϵ up to the finite terms, i.e. contributions of order $\epsilon^0 L^4$ and $\epsilon^0 L^3$. Instead, the one-loop corrections are expanded up to order ϵ^2 , i.e. including terms of order $\epsilon^2 L^4$ and $\epsilon^2 L^3$. As we will see, these higher-order terms in the ϵ -expansion must be taken into account in the relation between one- and two-loop mass singularities.

²These logarithms are evaluated in the Euclidean region $-s \gg M_W^2$, where the corrections are real. The imaginary parts that arise in the physical region (2.8) can be obtained via analytic continuation replacing s by $s + i0$.

In general, we have also logarithms

$$l_{\mu_i} := \log \left(\frac{\mu_i^2}{M_W^2} \right), \quad (2.12)$$

which depend on the renormalization scales $\mu_i = \mu_w, \mu_e$ of the weak mixing angle and the electromagnetic coupling constant. In the expansion (2.11), such logarithms are counted with the same weight as L , i.e. the terms of type $\epsilon^k l_{\mu_i}^m L^{j+k-m}$ are considered to be of the same order as $\epsilon^k L^{j+k}$. Moreover, since the heavy-particle masses are of the same order,

$$M_W \sim M_Z \sim m_t \sim M_H, \quad (2.13)$$

but not equal, the coefficients $\delta F_{\sigma;j,k}^{(l)}$ in (2.11) depend also on the ratios of these masses³. Actually, as we will see in the final result, they depend only on logarithms of the type

$$l_i := \log \left(\frac{M_i^2}{M_W^2} \right). \quad (2.14)$$

These logarithms are small compared to (2.10), and in principle one could neglect them, i.e. one could regard the equal-mass case (2.9), where they vanish, as a good approximation of the final result. However, we find that this equal-mass approximation cannot be adopted in order to simplify the analytical evaluation of the two-loop diagrams. In fact, as we will discuss in Sect. 5.1.5, certain two-loop integrals yield contributions that depend not logarithmically but linearly on the ratio M_W^2/M_Z^2 . In this case, the relation between the weak-boson masses and the weak mixing angle must be carefully taken into account in order not to destroy cancellations that guarantee the correct infrared behaviour of the two-loop corrections. This means that one cannot perform the diagrammatic calculation by using the same mass in all heavy-particle propagators.

2.4 Gauge interactions, symmetry breaking and mixing

For the Feynman rules we adopt the formalism of Ref. [13] (see App. B), which has been introduced in order to facilitate calculations in the high-energy limit of the spontaneously broken EW theory and permits, in particular, to make extensive use of various group-theoretical identities that can be found in App. A of Ref. [13]. In order to make the reader familiar with this formalism, we briefly review those aspects of spontaneous symmetry breaking that play a crucial role in the present calculation.

Within the unbroken phase of the EW theory, the gauge interactions are generated by the covariant derivative

$$\mathcal{D}_\mu = \partial_\mu - ie \sum_{\tilde{V}=W^1, W^2, W^3, B} \tilde{V}_\mu \tilde{I}^{\tilde{V}}, \quad (2.15)$$

where the vector bosons W^1, W^2, W^3 and B are associated to the generators

$$e\tilde{I}^{W^a} = g_2 T^a, \quad e\tilde{I}^B = -g_1 \frac{Y}{2}, \quad (2.16)$$

³This dependence starts at the subleading level, i.e. for $j \leq 2l - 1$.

of the $SU(2) \times U(1)$ symmetry group with the corresponding coupling constants g_2 and g_1 . The symmetry is spontaneously broken by a scalar Higgs doublet

$$\Phi = \begin{pmatrix} \phi^+ \\ \frac{1}{\sqrt{2}}(\mathbf{v} + H + i\chi) \end{pmatrix} \quad (2.17)$$

which acquires a vacuum expectation value (vev) \mathbf{v} corresponding to the minimum of its potential. The Higgs doublet is parametrized in terms of the four degrees of freedom $\Phi_i = \phi^+, \phi^-, H, \chi$, where $\phi^- = (\phi^+)^+$. In this representation the gauge-group generators are 4×4 matrices with components $\tilde{I}_{\Phi_i \Phi_j}^V$. The interactions of the gauge bosons with the vev generate the vector-boson mass matrix

$$M_{V\tilde{V}'}^2 = \frac{1}{2}e^2 \mathbf{v}^2 \left\{ \tilde{I}^V, \tilde{I}^{\tilde{V}'} \right\}_{HH}, \quad (2.18)$$

where the curly brackets denote an anticommutator. The physical gauge bosons A , Z , and W^\pm , are the mass eigenstates of this matrix, which result from the unitary transformation

$$W_\mu^\pm = \frac{1}{\sqrt{2}} (W_\mu^1 \mp iW_\mu^2), \quad Z_\mu = c_W W_\mu^3 + s_W B_\mu, \quad A_\mu = -s_W W_\mu^3 + c_W B_\mu, \quad (2.19)$$

where $c_W = \cos \theta_W$, $s_W = \sin \theta_W$, and θ_W is the weak mixing angle. Their masses are

$$M_{W^\pm} = \frac{1}{2}g_2 \mathbf{v}, \quad M_Z = \frac{1}{2c_W}g_2 \mathbf{v}, \quad M_A = 0, \quad (2.20)$$

and θ_W is related to the weak-boson masses via

$$M_W = c_W M_Z. \quad (2.21)$$

The vanishing mass of the photon is connected to the fact that the electric charge of the vev is zero. This provides the relation

$$c_W g_1 Y_\Phi = s_W g_2, \quad (2.22)$$

between the weak mixing angle, the coupling constants g_1 , g_2 and the hypercharge Y_Φ of the Higgs doublet. In the calculation we keep Y_Φ as a free parameter, which determines the degree of mixing in the gauge sector. This permits us to consider the Standard Model case, $Y_\Phi = 1$, as well as the special case $Y_\Phi = 0$ corresponding to an unmixed theory with

$$s_W = 0, \quad c_W = 1, \quad Z_\mu = W_\mu^3, \quad A_\mu = B_\mu, \quad M_W = M_Z. \quad (2.23)$$

In general, the mass-eigenstate gauge bosons are associated to the generators

$$eI^\pm = \frac{g_2}{\sqrt{2}} (T^1 \pm iT^2), \quad eI^Z = c_W g_2 T^3 - s_W g_1 \frac{Y}{2}, \quad eI^A = -s_W g_2 T^3 - c_W g_1 \frac{Y}{2} \quad (2.24)$$

with commutation relations

$$e [I^{V_1}, I^{V_2}] = ig_2 \sum_{V_3=A,Z,W^\pm} \varepsilon^{V_1 V_2 V_3} I^{\bar{V}_3}, \quad (2.25)$$

where \bar{V} denotes the complex conjugate of V ,

$$\varepsilon^{V_1 V_2 V_3} = i \times \begin{cases} (-1)^{p+1} c_w & \text{if } V_1 V_2 V_3 = \pi(Z W^+ W^-), \\ (-1)^p s_w & \text{if } V_1 V_2 V_3 = \pi(A W^+ W^-), \\ 0 & \text{otherwise,} \end{cases} \quad (2.26)$$

and $(-1)^p$ represents the sign of the permutation π . It is also useful to introduce the 4×4 matrices

$$\delta^{\text{SU}(2)} = \begin{pmatrix} s_w^2 & -s_w c_w & 0 & 0 \\ -s_w c_w & c_w^2 & 0 & 0 \\ 0 & 0 & 1 & 0 \\ 0 & 0 & 0 & 1 \end{pmatrix}, \quad \delta^{\text{U}(1)} = \begin{pmatrix} c_w^2 & s_w c_w & 0 & 0 \\ s_w c_w & s_w^2 & 0 & 0 \\ 0 & 0 & 0 & 0 \\ 0 & 0 & 0 & 0 \end{pmatrix}, \quad (2.27)$$

which project on the SU(2) and U(1) components of the gauge fields, respectively⁴. Analogously to the SU(2) structure constants, the ε tensor (2.26) satisfies the identities

$$\begin{aligned} \sum_{V_3=A,Z,W^\pm} \varepsilon^{\bar{V}_1 \bar{V}_2 \bar{V}_3} \varepsilon^{V'_1 V'_2 V'_3} &= \delta_{V_1 V'_1}^{\text{SU}(2)} \delta_{V_2 V'_2}^{\text{SU}(2)} - \delta_{V_1 V'_2}^{\text{SU}(2)} \delta_{V_2 V'_1}^{\text{SU}(2)}, \\ \sum_{V_2, V_3=A,Z,W^\pm} \varepsilon^{\bar{V}_1 \bar{V}_2 \bar{V}_3} \varepsilon^{V'_1 V'_2 V'_3} &= C_A \delta_{V_1 V'_1}^{\text{SU}(2)}, \end{aligned} \quad (2.28)$$

where $C_A = 2$ is the eigenvalue of the Casimir operator in the adjoint representation. The dimension of the SU(2) gauge group is denoted as $d_2 = \text{Tr}[\delta^{\text{SU}(2)}] = 3$.

The above group-theoretical identities have been used in the calculation in order to express all combinations of (non-commuting) fermionic chiral couplings I_σ^V occurring in Feynman diagrams in terms of the electric charge $Q = -I^A$, the diagonal matrices Y_σ, T_σ^3 , and the SU(2) Casimir operator C_σ , with $C_+ = 0$ and $C_- = 3/4$.

2.5 Mass-gap effects

The EW corrections depend on various mass scales: the masses of the heavy virtual particles, which we generically denote as $M_i = M_w, M_z, m_t, M_h$, and in general also a photon mass λ , which can be used to regularize mass singularities from virtual photons,

$$\delta F_\sigma^{(l)} \equiv \delta F_\sigma^{(l)}(\{M_i\}, \lambda). \quad (2.29)$$

⁴The order of the components $\delta_{VV'}^{\text{SU}(2)}$ and $\delta_{VV'}^{\text{U}(1)}$ in (2.27) corresponds to $V, V' = A, Z, W^+, W^-$. For instance we can project the SU(2) and U(1) contributions to the generators with

$$e \sum_{V=A,Z,W^\pm} \delta_{AV}^{\text{SU}(2)} I^V = -g_2 s_w T^3, \quad e \sum_{V=A,Z,W^\pm} \delta_{ZV}^{\text{SU}(2)} I^V = g_2 c_w T^3,$$

and

$$e \sum_{V=A,Z,W^\pm} \delta_{AV}^{\text{U}(1)} I^{\bar{V}} = -g_1 c_w \frac{Y}{2}, \quad e \sum_{V=A,Z,W^\pm} \delta_{ZV}^{\text{U}(1)} I^{\bar{V}} = -g_1 s_w \frac{Y}{2}.$$

In our calculation the photon and the light fermions are massless, and the heavy masses (2.13) are assumed to be of the same order but not equal. One of our aims is to investigate the effects resulting from the splittings between these masses, and in particular from the gap between the photon mass ($\lambda = 0$) and the weak-boson masses, which is a non-trivial aspect of the EW corrections. To this end, it is useful to isolate the mass-gap effects by adding and subtracting an equal-mass contribution, where the EW corrections are evaluated by setting $M_i = M_W$ and $\lambda = M_W$ in the propagators of the heavy particles and of the photon. This results in the splitting

$$\delta F_\sigma^{(l)}(\{M_i\}, 0) = \delta F_\sigma^{(l)}(\{M_i\}, M_W) \Big|_{M_i=M_W} + \Delta \delta F_\sigma^{(l)}(\{M_i\}, 0), \quad (2.30)$$

where all mass-gap effects, and in particular all infrared divergences (or combinations of infrared and ultraviolet divergences), are isolated in the subtracted term $\Delta \delta F_\sigma^{(l)}$, whereas the purely ultraviolet divergences are contained in the equal-mass term. According to the IREE, the equal-mass term is expected to behave as in a symmetric $SU(2) \times U(1)$ theory, whereas the mass-gap term, or more precisely the part resulting from the gap between the photon and the weak-boson masses, is expected to be of QED nature.

The analytical results for one- and two-loop diagrams that we present in the next sections are systematically split as in (2.30). The relevant loop integrals D_i and corresponding subtracted functions ΔD_i are defined in App. A. In all diagrams, the photonic couplings which occur in the equal-mass contributions are always written in terms of Y and T^3 , whereas in the mass-gap contributions we always write Q . This permits us, at the end of the calculation, to switch off all contributions originating from the A – W mass gap, i.e. to set $\lambda = M_W$, by simply substituting $Q = 0$.

The integration of the massive one- and two-loop integrals has been performed to NLL accuracy by means of an automatized algorithm based on the so-called sector-decomposition technique [27, 28, 29, 30]. This method permits to separate overlapping ultraviolet and mass singularities in Feynman-parameter integrals. As a result of this sector decomposition, the integrand can be split into simple subtraction terms that lead to ultraviolet and mass singularities and a finite remainder. Finally, the mass-singular integration of the subtraction terms that lead to the LL and NLL contributions can be performed in analytic form. A detailed description of the sector-decomposition algorithm for massive loop integrals is postponed to a forthcoming paper [31].

3 One-loop form factors

In this section we present the one-loop contributions to the bare and renormalized form factors (2.4). Each result is expanded in ϵ up to the order ϵ^2 .

3.1 Bare form factors

At one loop only the following topology contributes

$$\bar{P}_\sigma^{(1)} = e^2 F_\sigma^{(0)} \sum_{a_1=A,Z,\pm} I_\sigma^{\bar{a}_1} I_\sigma^{a_1} D_0(M_{a_1}). \quad (3.1)$$

The corresponding loop integral D_0 is defined in (A.6) and to NLL accuracy yields

$$\begin{aligned} D_0(M_W) &\stackrel{\text{NLL}}{=} -L^2 - \frac{2}{3}L^3\epsilon - \frac{1}{4}L^4\epsilon^2 + \epsilon^{-1} + 4L + 2L^2\epsilon + \frac{2}{3}L^3\epsilon^2, \\ \Delta D_0(M_Z) &\stackrel{\text{NLL}}{=} (2L + 2L^2\epsilon + L^3\epsilon^2) l_Z, \\ \Delta D_0(0) &\stackrel{\text{NLL}}{=} -2\epsilon^{-2} + L^2 + \frac{2}{3}L^3\epsilon + \frac{1}{4}L^4\epsilon^2 - 4\epsilon^{-1} - 4L - 2L^2\epsilon - \frac{2}{3}L^3\epsilon^2. \end{aligned} \quad (3.2)$$

This leads to

$$e^2 \delta F_{\sigma,0}^{(1)} = K_{\sigma,0}^{\text{sew}} D_0(M_W) + K_{\sigma,0}^Z \Delta D_0(M_Z) + K_{\sigma,0}^A \Delta D_0(0), \quad (3.3)$$

where

$$\begin{aligned} K_{\sigma,0}^{\text{sew}} &= e^2 \sum_{a_1=A,Z,\pm} I_\sigma^{\bar{a}_1} I_\sigma^{a_1} = g_1^2 \left(\frac{Y_\sigma}{2} \right)^2 + g_2^2 C_\sigma, \\ K_{\sigma,0}^Z &= e^2 I_\sigma^Z I_\sigma^Z = g_1^2 \left(\frac{Y_\sigma}{2} \right)^2 + g_2^2 (T_\sigma^3)^2 - e^2 Q^2, \quad K_{\sigma,0}^A = e^2 Q^2. \end{aligned} \quad (3.4)$$

3.2 Renormalization

The tree-level form factors $F_\sigma^{(0)}$ do not depend on the EW coupling constants and masses. Therefore, the only one-loop counterterm contribution arises from the on-shell wave-function renormalization constants (WFRC's) for massless chiral fermions⁵,

$$Z_\sigma = 1 + \sum_{l=1}^{\infty} \left(\frac{\alpha}{4\pi} \right)^l N_\epsilon^l \delta Z_\sigma^{(l)}, \quad (3.5)$$

which yield

$$\delta^{\text{WF}} F_\sigma^{(1)} = \delta Z_\sigma^{(1)}. \quad (3.6)$$

The one-loop WFRC's receive contributions only from massive weak bosons, whereas the photonic contribution vanishes owing to a cancellation between ultraviolet and mass singularities within dimensional regularization. To NLL accuracy we have

$$\begin{aligned} e^2 \delta Z_\sigma^{(1)} &\stackrel{\text{NLL}}{=} -\frac{1}{\epsilon} \sum_{a \neq A} e^2 I_\sigma^{\bar{a}} I_\sigma^a \left(\frac{-s}{M_a^2} \right)^\epsilon \\ &= -\frac{1}{\epsilon} \left\{ g_2^2 \left[C_\sigma - (T_\sigma^3)^2 \right] \left(\frac{-s}{M_W^2} \right)^\epsilon + \left[g_1^2 \left(\frac{Y_\sigma}{2} \right)^2 + g_2^2 (T_\sigma^3)^2 - e^2 Q^2 \right] \left(\frac{-s}{M_Z^2} \right)^\epsilon \right\}. \end{aligned} \quad (3.7)$$

⁵Note that we adopt a perturbative expansion with the same normalization factor N_ϵ as in (2.6).

3.3 Renormalized one-loop form factors

Combining the above results we obtain the renormalized one-loop form factors

$$\begin{aligned} e^2 \delta F_\sigma^{(1)} &= e^2 \left[\delta F_{\sigma,0}^{(1)} + \delta^{\text{WF}} F_\sigma^{(1)} \right] \\ &\stackrel{\text{NLL}}{=} K_{\sigma,0}^{\text{sew}} I(\epsilon, M_W) + K_{\sigma,0}^Z \Delta I(\epsilon, M_Z) + K_{\sigma,0}^A \Delta I(\epsilon, 0), \end{aligned} \quad (3.8)$$

where expanding in ϵ up to the order ϵ^2 we have

$$\begin{aligned} I(\epsilon, M_W) &\stackrel{\text{NLL}}{=} -L^2 - \frac{2}{3} L^3 \epsilon - \frac{1}{4} L^4 \epsilon^2 + 3L + \frac{3}{2} L^2 \epsilon + \frac{1}{2} L^3 \epsilon^2 + \mathcal{O}(\epsilon^3), \\ I(\epsilon, M_Z) &\stackrel{\text{NLL}}{=} I(\epsilon, M_W) + \text{I}_Z \left(2L + 2L^2 \epsilon + L^3 \epsilon^2 \right) + \mathcal{O}(\epsilon^3), \\ I(\epsilon, 0) &\stackrel{\text{NLL}}{=} -2\epsilon^{-2} - 3\epsilon^{-1}, \end{aligned} \quad (3.9)$$

and the subtracted functions ΔI are defined as

$$\Delta I(\epsilon, m) := I(\epsilon, m) - I(\epsilon, M_W). \quad (3.10)$$

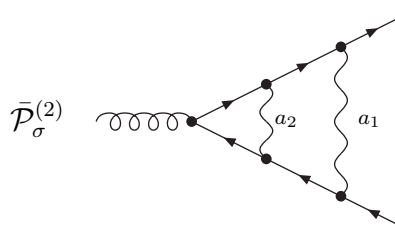
4 Two-loop form factors

In this section we present the two-loop contributions from individual Feynman diagrams and counterterms. Each result is expanded in ϵ up to the order ϵ^0 . The diagrams 1–3 in Sect. 4.1 give rise to LL’s and NLL’s, whereas all other diagrams and counterterm contributions yield only NLL’s.

4.1 Bare form factors

The two-loop Feynman diagrams contributing to the bare form factors involve virtual gauge bosons ($a_i = A, Z, W^\pm, \bar{a}_i = \bar{A}, \bar{Z}, \bar{W}^\pm$), ghosts ($u_i^a = u^A, u^Z, u^{W^\pm}$), Higgs bosons and would-be Goldstone bosons ($\Phi_i = H, \chi, \phi^\pm$), as well as fermionic doublets ($\Psi_i = u, d$). The corresponding loop integrals are defined in App. A. The computation is performed within the ’t Hooft–Feynman gauge, where the masses of the ghosts and would-be-Goldstone bosons read $M_{\phi^\pm} = M_{u^\pm} = M_W$ and $M_\chi = M_{u^Z} = M_Z$. The symbol M_i is used to denote generic heavy masses, i.e. $M_i = M_W, M_Z, m_t, M_H$.

4.1.1 Diagram 1



$$\bar{\mathcal{P}}_\sigma^{(2)} \quad \text{Diagram 1} = e^4 F_\sigma^{(0)} \sum_{a_1, a_2 = A, Z, \pm} I_\sigma^{\bar{a}_1} I_\sigma^{\bar{a}_2} I_\sigma^{a_2} I_\sigma^{a_1} D_1(M_{a_1}, M_{a_2}), \quad (4.1)$$

where the loop integral D_1 is defined in (A.6) and yields

$$\begin{aligned}
D_1(M_W, M_W) &\stackrel{\text{NLL}}{=} \frac{1}{6}L^4 - L^2\epsilon^{-1} - 2L^3, \\
\Delta D_1(M_1, M_2) &\stackrel{\text{NLL}}{=} -\frac{2}{3}L^3 l_1, \\
\Delta D_1(0, M_2) &\stackrel{\text{NLL}}{=} 2L^2\epsilon^{-2} + \frac{8}{3}L^3\epsilon^{-1} + \frac{11}{6}L^4 - 2\epsilon^{-3} - (8 + 4l_2)L\epsilon^{-2} \\
&\quad - (7 + 8l_2)L^2\epsilon^{-1} - \left(\frac{10}{3} + 8l_2\right)L^3, \\
\Delta D_1(M_1, 0) &\stackrel{\text{NLL}}{=} -\frac{2}{3}L^3 l_1, \\
\Delta D_1(0, 0) &\stackrel{\text{NLL}}{=} \epsilon^{-4} - \frac{1}{6}L^4 + 2\epsilon^{-3} + L^2\epsilon^{-1} + 2L^3.
\end{aligned} \tag{4.2}$$

This leads to

$$\begin{aligned}
e^4 \delta F_{\sigma,1}^{(2)} &\stackrel{\text{NLL}}{=} K_{\sigma,1}^{\text{sew}} D_1(M_W, M_W) + K_{\sigma,1}^Z \Delta D_1(M_Z, M_W) + K_{\sigma,1}^{AW} \Delta D_1(0, M_W) \\
&\quad + K_{\sigma,1}^{AZ} \Delta D_1(0, M_Z) + K_{\sigma,1}^{AA} \Delta D_1(0, 0),
\end{aligned} \tag{4.3}$$

where

$$\begin{aligned}
K_{\sigma,1}^{\text{sew}} &= e^4 \sum_{a_1, a_2 = A, Z, \pm} I_{\sigma}^{\bar{a}_1} I_{\sigma}^{\bar{a}_2} I_{\sigma}^{a_2} I_{\sigma}^{a_1} = \left[g_1^2 \left(\frac{Y_{\sigma}}{2} \right)^2 + g_2^2 C_{\sigma} \right]^2, \\
K_{\sigma,1}^Z &= e^4 \sum_{a_2 = A, Z, \pm} I_{\sigma}^Z I_{\sigma}^{\bar{a}_2} I_{\sigma}^{a_2} I_{\sigma}^Z = e^2 \left(I_{\sigma}^Z \right)^2 \left[g_1^2 \left(\frac{Y_{\sigma}}{2} \right)^2 + g_2^2 C_{\sigma} \right], \\
K_{\sigma,1}^{AW} &= e^4 \sum_{a_2 = \pm} I_{\sigma}^A I_{\sigma}^{\bar{a}_2} I_{\sigma}^{a_2} I_{\sigma}^A = e^2 g_2^2 Q^2 \left[C_{\sigma} - (T_{\sigma}^3)^2 \right], \\
K_{\sigma,1}^{AZ} &= e^4 Q^2 \left(I_{\sigma}^Z \right)^2, \quad K_{\sigma,1}^{AA} = e^4 Q^4.
\end{aligned} \tag{4.4}$$

Note that all ΔD -contributions from diagrams with $a_1 = Z, \pm$ and $a_2 = A, Z, \pm$ have been combined in the term proportional to $K_{\sigma,1}^Z$ in (4.3) using the relations

$$\begin{aligned}
\Delta D_1(M_Z, M_W) &\stackrel{\text{NLL}}{=} \Delta D_1(M_Z, M_Z) \stackrel{\text{NLL}}{=} \Delta D_1(M_Z, 0), \\
\Delta D_1(M_W, M_W) &\stackrel{\text{NLL}}{=} \Delta D_1(M_W, M_Z) \stackrel{\text{NLL}}{=} \Delta D_1(M_W, 0) \stackrel{\text{NLL}}{=} 0,
\end{aligned} \tag{4.5}$$

which can be read off from (4.2). For the diagrams that we present in the following similar simplifications are implicitly understood.

4.1.2 Diagram 2

$$\begin{aligned}
\bar{\mathcal{P}}_{\sigma}^{(2)} \quad \text{---} \text{---} \text{---} \text{---} \text{---} &= e^4 F_{\sigma}^{(0)} \sum_{a_1, a_2 = A, Z, \pm} I_{\sigma}^{\bar{a}_1} I_{\sigma}^{\bar{a}_2} I_{\sigma}^{a_1} I_{\sigma}^{a_2} D_2(M_{a_1}, M_{a_2}),
\end{aligned} \tag{4.6}$$

where the loop integral D_2 is defined in (A.6) and yields

$$\begin{aligned}
D_2(M_W, M_W) &\stackrel{\text{NLL}}{=} \frac{1}{3}L^4 - \frac{8}{3}L^3, \\
\Delta D_2(M_1, M_2) &\stackrel{\text{NLL}}{=} -\frac{2}{3}L^3(l_1 + l_2), \\
\Delta D_2(0, M_2) &\stackrel{\text{NLL}}{=} -\frac{2}{3}L^3\epsilon^{-1} - \frac{7}{6}L^4 + (4 + 2l_2)L^2\epsilon^{-1} + \left(\frac{20}{3} + \frac{10l_2}{3}\right)L^3, \\
\Delta D_2(M_1, 0) &\stackrel{\text{NLL}}{=} -\frac{2}{3}L^3\epsilon^{-1} - \frac{7}{6}L^4 + (4 + 2l_1)L^2\epsilon^{-1} + \left(\frac{20}{3} + \frac{10l_1}{3}\right)L^3, \\
\Delta D_2(0, 0) &\stackrel{\text{NLL}}{=} \epsilon^{-4} - \frac{1}{3}L^4 + 4\epsilon^{-3} + \frac{8}{3}L^3.
\end{aligned} \tag{4.7}$$

This leads to

$$\begin{aligned}
e^4 \delta F_{\sigma,2}^{(2)} &\stackrel{\text{NLL}}{=} K_{\sigma,2}^{\text{sew}} D_2(M_W, M_W) + K_{\sigma,2}^{WZ} \Delta D_2(M_W, M_Z) + K_{\sigma,2}^{WA} \Delta D_2(M_W, 0) \\
&\quad + K_{\sigma,2}^{ZZ} \Delta D_2(M_Z, M_Z) + K_{\sigma,2}^{ZA} \Delta D_2(M_Z, 0) + K_{\sigma,2}^{AA} \Delta D_2(0, 0),
\end{aligned} \tag{4.8}$$

where

$$\begin{aligned}
K_{\sigma,2}^{\text{sew}} &= e^4 \sum_{a_1, a_2 = A, Z, \pm} I_{\sigma}^{\bar{a}_1} I_{\sigma}^{\bar{a}_2} I_{\sigma}^{a_1} I_{\sigma}^{a_2} = \left[g_1^2 \left(\frac{Y_{\sigma}}{2} \right)^2 + g_2^2 C_{\sigma} \right]^2 - \frac{1}{2} g_2^4 C_A C_{\sigma}, \\
K_{\sigma,2}^{WZ} &= e^4 \sum_{a_1 = \pm} \left(I_{\sigma}^{\bar{a}_1} I_{\sigma}^Z I_{\sigma}^{a_1} I_{\sigma}^Z + I_{\sigma}^Z I_{\sigma}^{\bar{a}_1} I_{\sigma}^Z I_{\sigma}^{a_1} \right) = 2e^2 g_2^2 \left(I_{\sigma}^Z \right)^2 \left[C_{\sigma} - (T_{\sigma}^3)^2 \right] \\
&\quad - e g_2^3 c_W C_A T_{\sigma}^3 I_{\sigma}^Z, \\
K_{\sigma,2}^{WA} &= e^4 \sum_{a_1 = \pm} \left(I_{\sigma}^{\bar{a}_1} I_{\sigma}^A I_{\sigma}^{a_1} I_{\sigma}^A + I_{\sigma}^A I_{\sigma}^{\bar{a}_1} I_{\sigma}^A I_{\sigma}^{a_1} \right) \\
&= 2e^2 g_2^2 Q^2 \left[C_{\sigma} - (T_{\sigma}^3)^2 \right] - e g_2^3 s_W C_A T_{\sigma}^3 Q, \\
K_{\sigma,2}^{ZZ} &= e^4 \left(I_{\sigma}^Z \right)^4, \quad K_{\sigma,2}^{ZA} = 2e^4 Q^2 \left(I_{\sigma}^Z \right)^2, \quad K_{\sigma,2}^{AA} = e^4 Q^4.
\end{aligned} \tag{4.9}$$

4.1.3 Diagrams 3

$$\begin{aligned}
&\bar{\mathcal{P}}_{\sigma}^{(2)} \text{ (diagram)} + \bar{\mathcal{P}}_{\sigma}^{(2)} \text{ (diagram)} = \\
&= -2ie^3 g_2 F_{\sigma}^{(0)} \sum_{a_1, a_2, a_3 = A, Z, \pm} \varepsilon^{a_1 a_2 a_3} I_{\sigma}^{\bar{a}_1} I_{\sigma}^{\bar{a}_2} I_{\sigma}^{\bar{a}_3} D_3(M_{a_1}, M_{a_2}, M_{a_3}),
\end{aligned} \tag{4.10}$$

where the ε tensor is defined in (2.26). The loop integral D_3 is defined in (A.6) and yields

$$D_3(M_W, M_W, M_W) \stackrel{\text{NLL}}{=} \frac{1}{6}L^4 - 3L^2\epsilon^{-1} - 5L^3,$$

$$\begin{aligned}
\Delta D_3(M_1, M_2, M_3) &\stackrel{\text{NLL}}{=} -\frac{1}{3}L^3(l_1 + l_3), \\
\Delta D_3(0, M_2, M_3) &\stackrel{\text{NLL}}{=} -\frac{1}{3}L^3\epsilon^{-1} - \frac{7}{12}L^4 + (2 + l_3)L^2\epsilon^{-1} + \left(\frac{10}{3} + \frac{5l_3}{3}\right)L^3, \\
\Delta D_3(M_1, 0, M_3) &\stackrel{\text{NLL}}{=} -\frac{1}{3}L^3(l_1 + l_3), \\
\Delta D_3(M_1, M_2, 0) &\stackrel{\text{NLL}}{=} -\frac{1}{3}L^3\epsilon^{-1} - \frac{7}{12}L^4 - 6\epsilon^{-3} - 6L\epsilon^{-2} + (1 + l_1)L^2\epsilon^{-1} \\
&\quad + \left(\frac{17}{3} + \frac{5l_1}{3}\right)L^3.
\end{aligned} \tag{4.11}$$

This leads to

$$\begin{aligned}
e^4 \delta F_{\sigma,3}^{(2)} &= K_{\sigma,3}^{\text{sew}} D_3(M_W, M_W, M_W) + K_{\sigma,3}^{AWW} \Delta D_3(0, M_W, M_W) \\
&\quad + K_{\sigma,3}^{WWA} \Delta D_3(M_W, M_W, 0) + K_{\sigma,3}^{ZWW} \Delta D_3(M_Z, M_W, M_W),
\end{aligned} \tag{4.12}$$

where

$$\begin{aligned}
K_{\sigma,3}^{\text{sew}} &= -2ie^3 g_2 \sum_{a_1, a_2, a_3 = A, Z, \pm} \varepsilon^{a_1 a_2 a_3} I_{\sigma}^{\bar{a}_1} I_{\sigma}^{\bar{a}_2} I_{\sigma}^{\bar{a}_3} = g_2^4 C_A C_{\sigma}, \\
K_{\sigma,3}^{AWW} &= -2ie^3 g_2 \sum_{a_2, a_3 = \pm} \varepsilon^{A a_2 a_3} I_{\sigma}^A I_{\sigma}^{\bar{a}_2} I_{\sigma}^{\bar{a}_3} = eg_2^3 s_W C_A Q T_{\sigma}^3, \\
K_{\sigma,3}^{WWA} &= -2ie^3 g_2 \sum_{a_1, a_2 = \pm} \varepsilon^{a_1 a_2 A} I_{\sigma}^{\bar{a}_1} I_{\sigma}^{\bar{a}_2} I_{\sigma}^A = K_{\sigma,3}^{AWW}, \\
K_{\sigma,3}^{ZWW} &= -2ie^3 g_2 \left(\sum_{a_2, a_3 = \pm} \varepsilon^{Z a_2 a_3} I_{\sigma}^Z I_{\sigma}^{\bar{a}_2} I_{\sigma}^{\bar{a}_3} + \sum_{a_1, a_2 = \pm} \varepsilon^{a_1 a_2 Z} I_{\sigma}^{\bar{a}_1} I_{\sigma}^{\bar{a}_2} I_{\sigma}^Z \right) \\
&= 2eg_2^3 c_W C_A I_{\sigma}^Z T_{\sigma}^3.
\end{aligned} \tag{4.13}$$

4.1.4 Diagrams 4

$$\begin{aligned}
&\bar{\mathcal{P}}_{\sigma}^{(2)} \text{---} \textcirclearrowleft \textcirclearrowleft \textcirclearrowleft \textcirclearrowleft + \bar{\mathcal{P}}_{\sigma}^{(2)} \text{---} \textcirclearrowleft \textcirclearrowleft \textcirclearrowleft \textcirclearrowleft = \\
&= 2e^4 F_{\sigma}^{(0)} \sum_{a_1, a_2 = A, Z, \pm} I_{\sigma}^{\bar{a}_1} I_{\sigma}^{\bar{a}_2} I_{\sigma}^{a_2} I_{\sigma}^{a_1} D_4(M_{a_1}, M_{a_2}),
\end{aligned} \tag{4.14}$$

where the loop integral D_4 is defined in (A.6) and yields

$$\begin{aligned}
D_4(M_W, M_W) &\stackrel{\text{NLL}}{=} L^2\epsilon^{-1} + L^3, \\
\Delta D_4(M_1, M_2) &\stackrel{\text{NLL}}{=} 0,
\end{aligned}$$

$$\begin{aligned}
\Delta D_4(0, M_2) &\stackrel{\text{NLL}}{=} 2\epsilon^{-3} + 2L\epsilon^{-2} + L^2\epsilon^{-1} + \frac{1}{3}L^3, \\
\Delta D_4(M_1, 0) &\stackrel{\text{NLL}}{=} 0, \\
\Delta D_4(0, 0) &\stackrel{\text{NLL}}{=} \epsilon^{-3} - L^2\epsilon^{-1} - L^3.
\end{aligned} \tag{4.15}$$

This leads to

$$e^4 \delta F_{\sigma,4}^{(2)} = K_{\sigma,4}^{\text{sew}} D_4(M_W, M_W) + K_{\sigma,4}^{AV} \Delta D_4(0, M_W) + K_{\sigma,4}^{AA} \Delta D_4(0, 0), \tag{4.16}$$

where

$$\begin{aligned}
K_{\sigma,4}^{\text{sew}} &= 2e^4 \sum_{a_1, a_2 = A, Z, \pm} I_{\sigma}^{\bar{a}_1} I_{\sigma}^{\bar{a}_2} I_{\sigma}^{a_2} I_{\sigma}^{a_1} = 2 \left[g_1^2 \left(\frac{Y_{\sigma}}{2} \right)^2 + g_2^2 C_{\sigma} \right]^2, \\
K_{\sigma,4}^{AV} &= 2e^4 \sum_{a_2 \neq A} I_{\sigma}^A I_{\sigma}^{\bar{a}_2} I_{\sigma}^{a_2} I_{\sigma}^A = 2e^2 Q^2 \left[g_1^2 \left(\frac{Y_{\sigma}}{2} \right)^2 + g_2^2 C_{\sigma} - e^2 Q^2 \right], \\
K_{\sigma,4}^{AA} &= 2e^4 Q^4.
\end{aligned} \tag{4.17}$$

4.1.5 Diagrams 5

$$\begin{aligned}
&= 2e^4 F_{\sigma}^{(0)} \sum_{a_1, a_2 = A, Z, \pm} I_{\sigma}^{\bar{a}_2} I_{\sigma}^{\bar{a}_1} I_{\sigma}^{a_2} I_{\sigma}^{a_1} D_5(M_{a_1}, M_{a_2}),
\end{aligned} \tag{4.18}$$

where the loop integral D_5 is defined in (A.6) and yields

$$\begin{aligned}
D_5(M_W, M_W) &\stackrel{\text{NLL}}{=} -L^2\epsilon^{-1} - L^3, \\
\Delta D_5(M_1, M_2) &\stackrel{\text{NLL}}{=} 0, \\
\Delta D_5(0, M_2) &\stackrel{\text{NLL}}{=} -2\epsilon^{-3} - 2L\epsilon^{-2} - L^2\epsilon^{-1} - \frac{1}{3}L^3, \\
\Delta D_5(M_1, 0) &\stackrel{\text{NLL}}{=} 0, \\
\Delta D_5(0, 0) &\stackrel{\text{NLL}}{=} -\epsilon^{-3} + L^2\epsilon^{-1} + L^3.
\end{aligned} \tag{4.19}$$

This leads to

$$e^4 \delta F_{\sigma,5}^{(2)} = K_{\sigma,5}^{\text{sew}} D_5(M_W, M_W) + K_{\sigma,5}^{AV} \Delta D_5(0, M_W) + K_{\sigma,5}^{AA} \Delta D_5(0, 0), \tag{4.20}$$

where

$$\begin{aligned}
K_{\sigma,5}^{\text{sew}} &= 2e^4 \sum_{a_1, a_2 = A, Z, \pm} I_{\sigma}^{\bar{a}_1} I_{\sigma}^{\bar{a}_2} I_{\sigma}^{a_1} I_{\sigma}^{a_2} = 2 \left[g_1^2 \left(\frac{Y_{\sigma}}{2} \right)^2 + g_2^2 C_{\sigma} \right]^2 - g_2^4 C_A C_{\sigma}, \\
K_{\sigma,5}^{AV} &= 2e^4 \sum_{a_2 \neq A} I_{\sigma}^A I_{\sigma}^{\bar{a}_2} I_{\sigma}^A I_{\sigma}^{a_2} = 2e^2 Q^2 \left[g_1^2 \left(\frac{Y_{\sigma}}{2} \right)^2 + g_2^2 C_{\sigma} - e^2 Q^2 \right] - e g_2^3 s_{\text{W}} C_A Q T_{\sigma}^3, \\
K_{\sigma,5}^{AA} &= 2e^4 Q^4.
\end{aligned} \tag{4.21}$$

4.1.6 Diagrams 6

$$\begin{aligned}
& \bar{\mathcal{P}}_{\sigma}^{(2)} \text{ (diagram 6a)} + \bar{\mathcal{P}}_{\sigma}^{(2)} \text{ (diagram 6b)} = \\
& = -\frac{1}{2} e^2 g_2^2 F_{\sigma}^{(0)} \sum_{a_1, a_2, a_3, a_4 = A, Z, \pm} \varepsilon^{a_1 \bar{a}_2 \bar{a}_3} \varepsilon^{a_4 a_2 a_3} I_{\sigma}^{\bar{a}_1} I_{\sigma}^{\bar{a}_4} D_6(M_{a_1}, M_{a_2}, M_{a_3}, M_{a_4}),
\end{aligned} \tag{4.22}$$

where the loop integral D_6 is defined in (A.6) and yields

$$\begin{aligned}
D_6(M_{\text{W}}, M_{\text{W}}, M_{\text{W}}, M_{\text{W}}) &\stackrel{\text{NLL}}{=} \frac{10}{3} L^2 \epsilon^{-1} + \frac{40}{9} L^3, \\
\Delta D_6(M_1, M_2, M_3, M_4) &\stackrel{\text{NLL}}{=} 0, \\
\Delta D_6(0, M_2, M_3, M_4) &\stackrel{\text{NLL}}{=} \left(\frac{M_2^2 + M_3^2}{2M_4^2} \right) \left[-16\epsilon^{-3} - 16L\epsilon^{-2} + \frac{32}{3} L^3 \right], \\
\Delta D_6(M_1, 0, M_3, M_4) &\stackrel{\text{NLL}}{=} 0, \\
\Delta D_6(M_1, M_2, 0, M_4) &\stackrel{\text{NLL}}{=} 0, \\
\Delta D_6(M_1, M_2, M_3, 0) &\stackrel{\text{NLL}}{=} \left(\frac{M_2^2 + M_3^2}{2M_1^2} \right) \left[-16\epsilon^{-3} - 16L\epsilon^{-2} + \frac{32}{3} L^3 \right], \\
\Delta D_6(0, M_2, M_3, 0) &\stackrel{\text{NLL}}{=} \frac{20}{3} \epsilon^{-3} + \frac{20}{3} L \epsilon^{-2} - \frac{40}{9} L^3.
\end{aligned} \tag{4.23}$$

This leads to

$$\begin{aligned}
e^4 \delta F_{\sigma,6}^{(2)} &= K_{\sigma,6}^{\text{sew}} D_6(M_{\text{W}}, M_{\text{W}}, M_{\text{W}}, M_{\text{W}}) + K_{\sigma,6}^{AZ} \Delta D_6(0, M_{\text{W}}, M_{\text{W}}, M_{\text{Z}}) \\
&\quad + K_{\sigma,6}^{AA} \Delta D_6(0, M_{\text{W}}, M_{\text{W}}, 0),
\end{aligned} \tag{4.24}$$

where

$$K_{\sigma,6}^{\text{sew}} = -\frac{1}{2} e^2 g_2^2 \sum_{a_1, a_2, a_3, a_4 = A, Z, \pm} \varepsilon^{a_1 \bar{a}_2 \bar{a}_3} \varepsilon^{a_4 a_2 a_3} I_{\sigma}^{\bar{a}_1} I_{\sigma}^{\bar{a}_4} = -\frac{1}{2} g_2^4 C_A C_{\sigma},$$

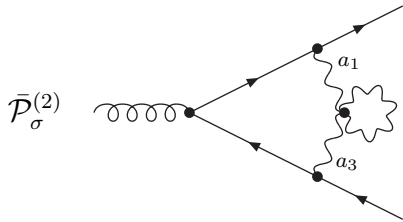
$$\begin{aligned}
K_{\sigma,6}^{AZ} &= -\frac{1}{2}e^2 g_2^2 \left[I_\sigma^A I_\sigma^Z \sum_{a_2,a_3=\pm} \varepsilon^{A\bar{a}_2\bar{a}_3} \varepsilon^{Za_2a_3} + (A \leftrightarrow Z) \right] = -e^2 g_2^2 s_W c_W C_A Q I_\sigma^Z, \\
K_{\sigma,6}^{AA} &= -\frac{1}{2}e^2 g_2^2 \sum_{a_2,a_3 \neq A} \varepsilon^{A\bar{a}_2\bar{a}_3} \varepsilon^{Aa_2a_3} I_\sigma^A I_\sigma^A = -\frac{1}{2}e^2 g_2^2 s_W^2 C_A Q^2.
\end{aligned} \tag{4.25}$$

We observe that the loop integrals associated with A-Z mixing-energy subdiagrams give rise to the contributions

$$\Delta D_6(0, M_W, M_W, M_Z) = \left(\frac{M_W}{M_Z} \right)^2 \left[-16\epsilon^{-3} - 16L\epsilon^{-2} + \frac{32}{3}L^3 \right], \tag{4.26}$$

which depend linearly on the ratio $(M_W/M_Z)^2$. This dependence appears also in all other bosonic A-Z mixing-energy diagrams 7–10 and is discussed in detail in Sect. 5.1.5. There we explain its origin and show that, in order not to destroy cancellations that ensure the correct infrared behaviour of the corrections, the relation (2.21) between the weak-boson masses and the weak mixing angle must be carefully taken into account. This means that such loop integrals cannot be evaluated using $M_W = M_Z$ in the weak-boson propagators.

4.1.7 Diagram 7



$$\bar{\mathcal{P}}_\sigma^{(2)} = e^2 g_2^2 F_\sigma^{(0)} \sum_{a_1, a_2, a_3 = A, Z, \pm} I_\sigma^{\bar{a}_1} I_\sigma^{\bar{a}_3} \left[\delta_{\bar{a}_1 a_3}^{\text{SU}(2)} \delta_{\bar{a}_2 a_2}^{\text{SU}(2)} - \delta_{\bar{a}_1 a_2}^{\text{SU}(2)} \delta_{\bar{a}_2 a_3}^{\text{SU}(2)} \right] \times (D-1) D_7(M_{a_1}, M_{a_2}, M_{a_3}),
\tag{4.27}$$

where $\delta^{\text{SU}(2)}$ is the matrix is defined in (2.27) and $D = 4 - 2\epsilon$. The loop integral D_7 is defined in (A.6) and yields

$$\begin{aligned}
D_7(M_W, M_W, M_W) &\stackrel{\text{NLL}}{=} 0, \\
\Delta D_7(M_1, M_2, M_3) &\stackrel{\text{NLL}}{=} 0, \\
\Delta D_7(0, M_2, M_3) &\stackrel{\text{NLL}}{=} \left(\frac{M_2}{M_3} \right)^2 \left[-2\epsilon^{-3} - 2L\epsilon^{-2} + \frac{4}{3}L^3 \right], \\
\Delta D_7(M_1, 0, M_3) &\stackrel{\text{NLL}}{=} 0, \\
\Delta D_7(M_1, M_2, 0) &\stackrel{\text{NLL}}{=} \left(\frac{M_2}{M_1} \right)^2 \left[-2\epsilon^{-3} - 2L\epsilon^{-2} + \frac{4}{3}L^3 \right], \\
\Delta D_7(0, M_2, 0) &\stackrel{\text{NLL}}{=} 0.
\end{aligned} \tag{4.28}$$

This leads to

$$e^4 \delta F_{\sigma,7}^{(2)} = K_{\sigma,7}^{AZ} \Delta D_7(0, M_W, M_Z), \tag{4.29}$$

where

$$\begin{aligned} K_{\sigma,7}^{AZ} &= (D-1)e^2 g_2^2 \left[I_{\sigma}^A I_{\sigma}^Z \sum_{a_2=\pm} \left(\delta_{AZ}^{\text{SU}(2)} \delta_{\bar{a}_2 a_2}^{\text{SU}(2)} - \delta_{Aa_2}^{\text{SU}(2)} \delta_{\bar{a}_2 Z}^{\text{SU}(2)} \right) + (A \leftrightarrow Z) \right] \\ &= 2(D-1)(d_2-1)e^2 g_2^2 s_{\text{W}} c_{\text{W}} Q I_{\sigma}^Z, \end{aligned} \quad (4.30)$$

and $d_2 = 3$ is the dimension of the $SU(2)$ group.

4.1.8 Diagram 8

$$\begin{aligned}
\bar{P}_\sigma^{(2)} \quad \text{Diagram: } &= e^6 \mathbf{v}^2 F_\sigma^{(0)} \sum_{a_1, a_3, a_4 = A, Z, \pm} I_\sigma^{\bar{a}_1} I_\sigma^{\bar{a}_4} \sum_{\Phi_{i_2} = H, \chi, \phi^\pm} \{I^{a_1}, I^{\bar{a}_3}\}_{H\Phi_{i_2}} \\
&\times \{I^{a_3}, I^{a_4}\}_{\Phi_{i_2} H} D_8(M_{a_1}, M_{\Phi_2}, M_{a_3}, M_{a_4}),
\end{aligned} \tag{4.31}$$

where the curly brackets denote anticommutators and \mathbf{v} is the vev. The loop integral D_8 is defined in (A.6) and yields

$$\begin{aligned}
& M_{\text{W}}^2 D_8(M_{\text{W}}, M_{\text{W}}, M_{\text{W}}, M_{\text{W}}) \stackrel{\text{NLL}}{=} 0, \\
& M_{\text{W}}^2 \Delta D_8(M_1, M_2, M_3, M_4) \stackrel{\text{NLL}}{=} 0, \\
& \Delta D_8(0, M_2, M_3, M_4) \stackrel{\text{NLL}}{=} \left(\frac{1}{M_4}\right)^2 \left[-2\epsilon^{-3} - 2L\epsilon^{-2} + \frac{4}{3}L^3 \right], \\
& M_{\text{W}}^2 D_8(M_1, M_2, 0, M_4) \stackrel{\text{NLL}}{=} 0, \\
& \Delta D_8(M_1, M_2, M_3, 0) \stackrel{\text{NLL}}{=} \left(\frac{1}{M_1}\right)^2 \left[-2\epsilon^{-3} - 2L\epsilon^{-2} + \frac{4}{3}L^3 \right], \\
& M_{\text{W}}^2 D_8(0, M_2, M_3, 0) \stackrel{\text{NLL}}{=} 0. \tag{4.32}
\end{aligned}$$

This leads to

$$e^4 \delta F_{\sigma,8}^{(2)} = K_{\sigma,8}^{AZ} \Delta D_8(0, M_W, M_W, M_Z), \quad (4.33)$$

where

$$\begin{aligned}
K_{\sigma,8}^{AZ} &= e^6 \mathbf{v}^2 \left[I_\sigma^A I_\sigma^Z \sum_{a_3=\pm} \sum_{\Phi_{i_2}=\phi^\pm} \left\{ I^A, I^{\bar{a}_3} \right\}_{H\Phi_{i_2}} \left\{ I^{a_3}, I^Z \right\}_{\Phi_{i_2} H} + (A \leftrightarrow Z) \right] \\
&= -\frac{1}{2} e^2 g_2^4 \frac{s_w}{c_w} \mathbf{v}^2 Q I_\sigma^Z \left[C_A - (d_2 - 1) c_w^2 \right]. \tag{4.34}
\end{aligned}$$

The above diagram is especially interesting since it represents the only contribution involving couplings proportional to v , which originate from spontaneous symmetry breaking. One could naively expect that contributions involving such couplings vanish in the

limit $\mathbf{v}^2/s \rightarrow 0$. However, in this case we see that the loop integrals associated to A–Z mixing-energy subdiagrams,

$$D_8(0, M_W, M_W, M_Z) \stackrel{\text{NLL}}{=} \left(\frac{1}{M_Z}\right)^2 \left[-2\epsilon^{-3} - 2L\epsilon^{-2} + \frac{4}{3}L^3 \right], \quad (4.35)$$

are inversely proportional to M_Z^2 . As a result, the above diagram provides a non-suppressed correction in the high-energy limit.

4.1.9 Diagram 9

$$\bar{\mathcal{P}}_\sigma^{(2)} \text{ (loop diagram)} = \frac{1}{2} e^4 F_\sigma^{(0)} \sum_{a_1, a_4 = A, Z, \pm} I_\sigma^{\bar{a}_1} I_\sigma^{\bar{a}_4} \sum_{\Phi_{i_2}, \Phi_{i_3} = H, \chi, \phi^\pm} I_{\Phi_{i_3} \Phi_{i_2}}^{a_1} I_{\Phi_{i_2} \Phi_{i_3}}^{a_4} \times D_9(M_{a_1}, M_{\Phi_{i_2}}, M_{\Phi_{i_3}}, M_{a_4}), \quad (4.36)$$

where the loop integral D_9 is defined in (A.6) and yields

$$\begin{aligned} D_9(M_W, M_W, M_W, M_W) &\stackrel{\text{NLL}}{=} \frac{1}{3} L^2 \epsilon^{-1} + \frac{4}{9} L^3, \\ \Delta D_9(M_1, M_2, M_3, M_4) &\stackrel{\text{NLL}}{=} 0, \\ \Delta D_9(0, M_2, M_3, M_4) &\stackrel{\text{NLL}}{=} \left(\frac{M_2^2 + M_3^2}{2M_4^2} \right) \left[4\epsilon^{-3} + 4L\epsilon^{-2} - \frac{8}{3}L^3 \right], \\ \Delta D_9(M_1, M_2, M_3, 0) &\stackrel{\text{NLL}}{=} \left(\frac{M_2^2 + M_3^2}{2M_1^2} \right) \left[4\epsilon^{-3} + 4L\epsilon^{-2} - \frac{8}{3}L^3 \right], \\ \Delta D_9(0, M_2, M_3, 0) &\stackrel{\text{NLL}}{=} \frac{2}{3}\epsilon^{-3} + \frac{2}{3}L\epsilon^{-2} - \frac{4}{9}L^3, \end{aligned} \quad (4.37)$$

for massive scalars inside the vacuum polarization⁶. This leads to

$$\begin{aligned} e^4 \delta F_{\sigma,9}^{(2)} &= K_{\sigma,9}^{\text{sew}} D_9(M_W, M_{\phi^\pm}, M_{\phi^\pm}, M_W) + K_{\sigma,9}^{AZ} \Delta D_9(0, M_{\phi^\pm}, M_{\phi^\pm}, M_Z) \\ &\quad + K_{\sigma,9}^{AA} \Delta D_9(0, M_{\phi^\pm}, M_{\phi^\pm}, 0), \end{aligned} \quad (4.38)$$

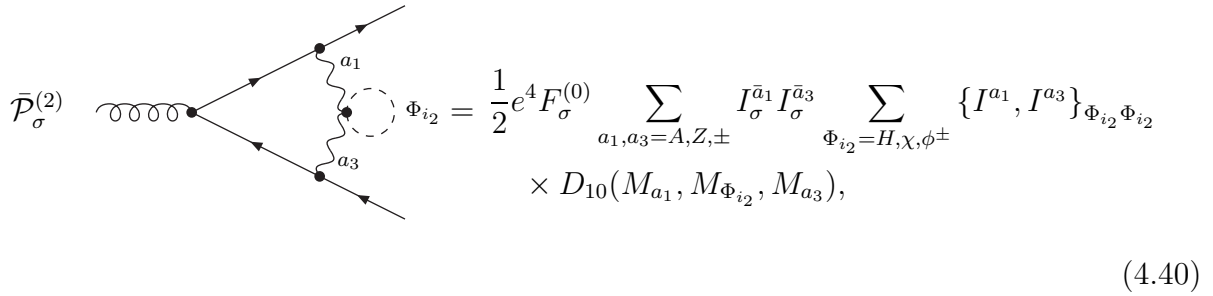
where

$$\begin{aligned} K_{\sigma,9}^{\text{sew}} &= e^4 \sum_{a_1, a_4 = A, Z, \pm} I_\sigma^{\bar{a}_1} I_\sigma^{\bar{a}_4} \text{Tr}_\Phi(I^{a_1} I^{a_4}) = g_1^4 \frac{Y_\Phi^2}{2} \left(\frac{Y_\sigma}{2} \right)^2 + \frac{1}{2} g_2^4 C_\sigma, \\ K_{\sigma,9}^{AZ} &= \frac{1}{2} e^4 \left[I_\sigma^A I_\sigma^Z \sum_{\Phi_{i_2}, \Phi_{i_3} = \phi^\pm} I_{\Phi_{i_3} \Phi_{i_2}}^A I_{\Phi_{i_2} \Phi_{i_3}}^Z + (A \leftrightarrow Z) \right] = -e^2 s_W c_W Q I_\sigma^Z \left(g_1^2 Y_\Phi^2 - g_2^2 \right), \\ K_{\sigma,9}^{AA} &= e^4 Q^2 \text{Tr}_\Phi(I^A I^A) = \frac{1}{2} e^2 Q^2 \left[g_1^2 c_W^2 Y_\Phi^2 + g_2^2 s_W^2 \right]. \end{aligned} \quad (4.39)$$

⁶For massless scalars inside the vacuum polarization we would obtain a result analogous to massless fermions (see Sect. 4.1.11): $4D_9(m_1, 0, 0, m_4) \stackrel{\text{NLL}}{=} D_{11,0}(m_1, 0, 0, m_4)$ for masses m_1, m_4 either equal to 0 or of the order of M_W .

The traces Tr_Φ in the above identities can be read off from (B.4).

4.1.10 Diagram 10



$$\bar{\mathcal{P}}_\sigma^{(2)} \text{ (wavy line)} = \frac{1}{2} e^4 F_\sigma^{(0)} \sum_{a_1, a_3 = A, Z, \pm} I_\sigma^{\bar{a}_1} I_\sigma^{\bar{a}_3} \sum_{\Phi_{i2} = H, \chi, \phi^\pm} \{I^{a_1}, I^{a_3}\}_{\Phi_{i2} \Phi_{i2}} \times D_{10}(M_{a_1}, M_{\Phi_{i2}}, M_{a_3}), \quad (4.40)$$

where $D_{10} \equiv D_7$. This leads to

$$e^4 \delta F_{\sigma,10}^{(2)} = K_{\sigma,10}^{AZ} \Delta D_7(0, M_{\phi^\pm}, M_Z), \quad (4.41)$$

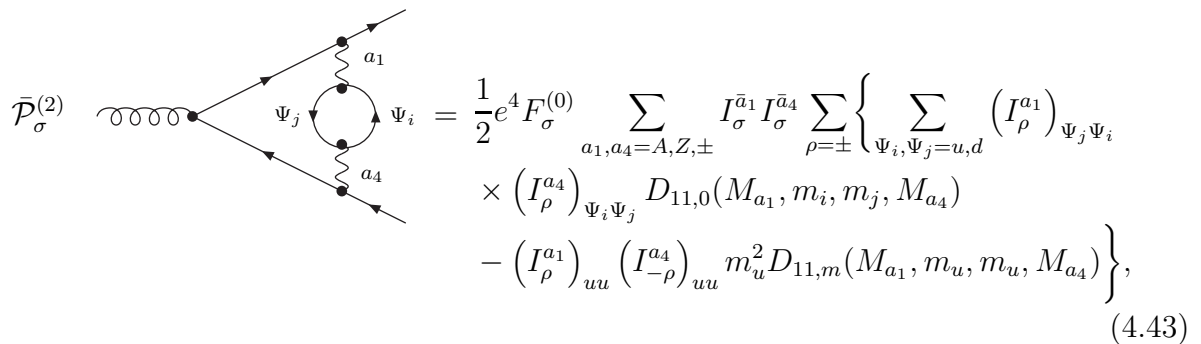
where

$$K_{\sigma,10}^{AZ} = \frac{1}{2} e^4 \left[I_\sigma^A I_\sigma^Z \sum_{\Phi_{i2} = \phi^\pm} \{I^A, I^Z\}_{\Phi_{i2} \Phi_{i2}} + (A \leftrightarrow Z) \right] = 2 K_{\sigma,9}^{AZ}. \quad (4.42)$$

Also this diagram, which yields NLL contributions only through A–Z mixing-energy subdiagrams, gives rise to a correction proportional to $(M_W/M_Z)^2$ via $\Delta D_7(0, M_{\phi^\pm}, M_Z)$. This correction cancels the contribution proportional to $(M_W/M_Z)^2$ that originates from diagram 9, i.e. the term $K_{\sigma,9}^{AZ} \Delta D_9$ in (4.38).

4.1.11 Diagram 11

Finally, we consider the contributions involving fermionic self-energy subdiagrams. Here we just consider a generic fermionic doublet Ψ with components $\Psi_i = u, d$. The sum over the three generations of leptons and quarks, as well as colour factors, are implicitly understood. Assuming that all down-type fermions are massless ($m_d = 0$) and that the masses of up-type fermions are $m_u = 0$ or m_t , we have



$$\bar{\mathcal{P}}_\sigma^{(2)} \text{ (wavy line)} = \frac{1}{2} e^4 F_\sigma^{(0)} \sum_{a_1, a_4 = A, Z, \pm} I_\sigma^{\bar{a}_1} I_\sigma^{\bar{a}_4} \sum_{\rho = \pm} \left\{ \sum_{\Psi_i, \Psi_j = u, d} (I_\rho^{a_1})_{\Psi_j \Psi_i} \times (I_\rho^{a_4})_{\Psi_i \Psi_j} D_{11,0}(M_{a_1}, m_i, m_j, M_{a_4}) - (I_\rho^{a_1})_{uu} (I_{-\rho}^{a_4})_{uu} m_u^2 D_{11,m}(M_{a_1}, m_u, m_u, M_{a_4}) \right\}, \quad (4.43)$$

where $D_{11,m} \equiv -4D_8$ represents the contribution associated to the m_u -terms in the numerator of the up-fermion propagators, whereas the integral $D_{11,0}$, which is defined in (A.6), accounts for the remaining contributions. This latter integral yields

$$\begin{aligned}
D_{11,0}(M_W, M_W, M_W, M_W) &\stackrel{\text{NLL}}{=} \frac{4}{3}L^2\epsilon^{-1} + \frac{16}{9}L^3, \\
\Delta D_{11,0}(M_1, m_2, m_3, M_4) &\stackrel{\text{NLL}}{=} 0, \\
\Delta D_{11,0}(0, m_2, m_3, M_4) &\stackrel{\text{NLL}}{=} \left(\frac{m_2^2 + m_3^2}{2M_4^2}\right) \left[8\epsilon^{-3} + 8L\epsilon^{-2} - \frac{16}{3}L^3\right], \\
\Delta D_{11,0}(M_1, m_2, m_3, 0) &\stackrel{\text{NLL}}{=} \left(\frac{m_2^2 + m_3^2}{2M_1^2}\right) \left[8\epsilon^{-3} + 8L\epsilon^{-2} - \frac{16}{3}L^3\right], \\
\Delta D_{11,0}(0, M_2, M_3, 0) &\stackrel{\text{NLL}}{=} \frac{8}{3}\epsilon^{-3} + \frac{8}{3}L\epsilon^{-2} - \frac{16}{9}L^3, \\
\Delta D_{11,0}(0, 0, 0, 0) &\stackrel{\text{NLL}}{=} \frac{2}{3}\epsilon^{-3} - \frac{4}{3}L^2\epsilon^{-1} - \frac{16}{9}L^3,
\end{aligned} \tag{4.44}$$

for masses $M_i \sim M_W$ and $m_2, m_3 = 0$ or m_t . Using the fact that

$$\Delta D_{11,0}(M_1, m_2, m_3, 0) = \frac{m_2^2 + m_3^2}{2} \Delta D_{11,m}(M_1, m_2, m_3, 0), \tag{4.45}$$

and a similar relation with $0 \leftrightarrow M_1$, we can write

$$\begin{aligned}
e^4 \delta F_{\sigma,11}^{(2)} &= K_{\sigma,11}^{\text{sew}} D_{11,0}(M_W, M_W, M_W, M_W) + K_{\sigma,11}^{AZ} m_u^2 \Delta D_{11,m}(0, m_u, m_u, M_Z) \\
&\quad + K_{\sigma,11}^{AA,0} \Delta D_{11,0}(0, 0, 0, 0) + K_{\sigma,11}^{AA,m} [\Delta D_{11,0}(0, m_u, m_u, 0) - \Delta D_{11,0}(0, 0, 0, 0)],
\end{aligned} \tag{4.46}$$

where⁷

$$\begin{aligned}
K_{\sigma,11}^{\text{sew}} &= \frac{1}{2} e^4 \sum_{a_1, a_4 = A, Z, \pm} I_{\sigma}^{\bar{a}_1} I_{\sigma}^{\bar{a}_4} \sum_{\rho = \pm} \text{Tr}_{\Psi} \left(I_{\rho}^{a_1} I_{\rho}^{a_4} \right) \\
&= \frac{1}{4} \left[g_1^4 \left(\frac{Y_{\sigma}}{2} \right)^2 \sum_{\rho = \pm} \frac{(Y_{\rho})_d^2 + (Y_{\rho})_u^2}{2} + g_2^4 C_{\sigma} \right], \\
K_{\sigma,11}^{AA,0} &= e^4 Q^2 (Q_u^2 + Q_d^2), \quad K_{\sigma,11}^{AA,m} = e^4 Q^2 Q_u^2,
\end{aligned} \tag{4.47}$$

and the trace Tr_{Ψ} can be read off from (B.4). The $m_u^2 \Delta D_{11,m}$ -term in (4.46) originates from A-Z mixing-energy contributions to the $D_{11,0}$ - and $m_u^2 D_{11,m}$ -terms in (4.43), which are proportional to $(m_u/M_Z)^2$. Their combination yields

$$K_{\sigma,11}^{AZ} = \frac{1}{2} e^4 I_{\sigma}^A I_{\sigma}^Z \sum_{\rho = \pm} \left[\left(I_{\rho}^A \right)_u \left(I_{\rho}^Z \right)_u - \left(I_{\rho}^A \right)_u \left(I_{-\rho}^Z \right)_u \right] + (A \leftrightarrow Z) = 0. \tag{4.48}$$

This means the NLL contributions proportional to $(m_u/M_Z)^2$ vanish owing to a cancellation between the momentum- and mass-terms in the fermionic propagators. This is analogous to the cancellation between the $(M_W/M_Z)^2$ -terms from A-Z mixing-energies in diagrams 9 and 10.

⁷For the generators of neutral-current interactions, $I^V = I^A, I^Z$, we write $(I_{\rho}^V)_{\Psi_i \Psi_j} = \delta_{\Psi_i \Psi_j} (I_{\rho}^V)_{\Psi_i}$. A similar notation is used for $Q_{\rho} = Q$ and for the hypercharge Y_{ρ} .

4.2 Renormalization

In this section we discuss the renormalization of the two-loop form factors. As we will see, to NLL accuracy only one-loop counterterms contribute. These counterterms are evaluated in a generic renormalization scheme, where the weak mixing angle and the electromagnetic coupling constant are renormalized at the scales μ_w and μ_e , respectively. The on-shell (OS) renormalization scheme⁸ corresponds to $\mu_w = M_W$ and $\mu_e \leq M_W$, whereas the minimal-subtraction (MS) scheme is simply obtained by setting $\mu_w = \mu_e = \mu_0$, where μ_0 is the scale of dimensional regularization. The one-loop mass and coupling-constant counterterms are expressed in terms of the β -function coefficients $b_1^{(1)}$, $b_2^{(1)}$, $b_e^{(1)}$, and $b_{\text{QED}}^{(1)}$, which are defined in App. B.

4.2.1 Mass renormalization

Since the tree-level form factors do not depend on the weak-boson masses, the only two-loop contributions resulting from the renormalization of the bare masses $M_{0,a}$ of the weak bosons $a = Z, W$,

$$M_{0,a} = M_a \left[1 + \sum_{l=1}^{\infty} \left(\frac{\alpha}{4\pi} \right)^l N_e^l \delta Z_{M_a}^{(l)} \right], \quad (4.49)$$

are

$$\delta^M F_{\sigma}^{(2)} = \sum_{a=Z,W} \delta Z_{M_a}^{(1)} \frac{\partial \delta F_{\sigma}^{(1)}}{\partial \log M_a}. \quad (4.50)$$

To NLL accuracy, the one-loop mass counterterms read

$$e^2 \delta Z_{M_a}^{(1)} \stackrel{\text{NLL}}{=} -\frac{1}{2} \left\{ e^2 b_{aa}^{(1)} - 4 \left[g_1^2 \left(\frac{Y_{\Phi}}{2} \right)^2 + g_2^2 C_{\Phi} \right] + g_2^2 \frac{3m_t^2}{2M_W^2} \right\} \frac{1}{\epsilon} \left(\frac{-s}{\mu_w^2} \right)^{\epsilon}, \quad (4.51)$$

where $b_{ZZ}^{(1)} = s_w^2 b_1^{(1)} + c_w^2 b_2^{(1)}$ and $b_{WW}^{(1)} = b_2^{(1)}$. In order to determine the degree of singularity of the two-loop mass-counterterm contribution (4.50), let us consider the LL contributions to the one-loop form factors,

$$\delta F_{\sigma}^{(1)} \sim M_a^j \epsilon^k \log^{2+k}(M_a), \quad (4.52)$$

where $k \geq -2$, and also mass-suppressed contributions are included by assuming $j \geq 0$. The terms resulting from a mass renormalization of (4.52) are of order

$$\delta^M F_{\sigma}^{(2)} \sim M_a^j \epsilon^k \left[(2+k) \log^{2+k-1}(M_a) + j \log^{2+k}(M_a) \right] \delta Z_{M_a}^{(1)} \quad (4.53)$$

and, as we see, only non-suppressed contributions with $j = 0$ or $j = \mathcal{O}(\epsilon)$ remain non-suppressed. Moreover, since the mass counterterms (4.51) provide only poles of order ϵ^{-1} , we conclude that the degree of singularity of (4.53) is only 2 and

$$\delta^M F_{\sigma}^{(2)} \stackrel{\text{NLL}}{=} 0. \quad (4.54)$$

⁸The NLL finite parts of the one-loop counterterms within the OS scheme can be found in Ref. [13].

4.2.2 Coupling-constant renormalization

Since the tree-level form factors do not depend on the EW coupling constants, the only two-loop contributions resulting from the renormalization

$$g_{0,i} = g_i + \sum_{l=1}^{\infty} \left(\frac{\alpha}{4\pi} \right)^l N_{\epsilon}^l \delta g_i^{(l)}, \quad e_0 = e + \sum_{l=1}^{\infty} \left(\frac{\alpha}{4\pi} \right)^l N_{\epsilon}^l \delta e^{(l)} \quad (4.55)$$

of the bare couplings $g_{0,1}$, $g_{0,2}$, and e_0 , are

$$e^2 \delta^{\text{CR}} F_{\sigma}^{(2)} = \left(\sum_{i=1}^2 \delta g_i^{(1)} \frac{\partial}{\partial g_i} + \delta e^{(1)} \frac{\partial}{\partial e} \right) \left[e^2 \delta F_{\sigma}^{(1)} \right]. \quad (4.56)$$

Within the on-shell scheme [32], the renormalized parameters e, g_1, g_2, c_w, M_Z , and M_W , are fixed by renormalization conditions for the electromagnetic charge and the weak-boson masses and through the relations (2.21), (2.22), and (2.24). The counterterms for the renormalization of the bare weak mixing angle,

$$c_{w,0} = c_w + \sum_{l=1}^{\infty} \left(\frac{\alpha}{4\pi} \right)^l N_{\epsilon}^l \delta c_w^{(l)}, \quad s_{w,0} = s_w + \sum_{l=1}^{\infty} \left(\frac{\alpha}{4\pi} \right)^l N_{\epsilon}^l \delta s_w^{(l)}, \quad (4.57)$$

result from the weak-boson mass counterterms (4.51) and read

$$\delta c_w^{(1)} \stackrel{\text{NLL}}{=} \frac{c_w s_w^2}{2} \left(b_1^{(1)} - b_2^{(1)} \right) \frac{1}{\epsilon} \left(\frac{-s}{\mu_w^2} \right)^{\epsilon}, \quad \delta s_w^{(1)} = -\frac{c_w}{s_w} \delta c_w^{(1)}. \quad (4.58)$$

The electric-charge renormalization at the scale $\mu_e \leq M_W$ yields

$$\delta e^{(1)} \stackrel{\text{NLL}}{=} -\frac{e}{2} \frac{1}{\epsilon} \left\{ b_e^{(1)} \left(\frac{-s}{\mu_w^2} \right)^{\epsilon} + b_{\text{QED}}^{(1)} \left[\left(\frac{-s}{\mu_e^2} \right)^{\epsilon} - \left(\frac{-s}{\mu_w^2} \right)^{\epsilon} \right] \right\}, \quad (4.59)$$

where the $b_e^{(1)}$ - and $b_{\text{QED}}^{(1)}$ -terms describe the running of the electromagnetic coupling above and below the electroweak scale, respectively. This latter is driven by light fermions only. The resulting counterterms for the gauge-couplings g_1 and g_2 , read

$$\delta g_i^{(1)} \stackrel{\text{NLL}}{=} -\frac{g_i}{2} \frac{1}{\epsilon} \left\{ b_i^{(1)} \left(\frac{-s}{\mu_w^2} \right)^{\epsilon} + b_{\text{QED}}^{(1)} \left[\left(\frac{-s}{\mu_e^2} \right)^{\epsilon} - \left(\frac{-s}{\mu_w^2} \right)^{\epsilon} \right] \right\}. \quad (4.60)$$

4.2.3 Wave-function renormalization

The fermionic WFRC's (3.5) yield the following two-loop counterterm-contributions

$$\delta^{\text{WF}} F_{\sigma}^{(2)} = \delta Z_{\sigma}^{(1)} \delta F_{\sigma}^{(1)} + \delta Z_{\sigma}^{(2)} - \left(\delta Z_{\sigma}^{(1)} \right)^2, \quad (4.61)$$

where $\delta F_{\sigma}^{(1)}$ are the renormalized one-loop form factors. Since both $\delta Z_{\sigma}^{(2)}$ and $\left(\delta Z_{\sigma}^{(1)} \right)^2$ provide only poles of order ϵ^{-2} , to NLL accuracy we simply have

$$\delta^{\text{WF}} F_{\sigma}^{(2)} \stackrel{\text{NLL}}{=} \delta Z_{\sigma}^{(1)} \delta F_{\sigma}^{(1)}, \quad (4.62)$$

and the one-loop WFRC's are given in (3.7).

4.3 Renormalized two-loop form factors

In this section, we present the results for the renormalized two-loop form factors

$$\delta F_\sigma^{(2)} \stackrel{\text{NLL}}{=} \sum_{i=1}^{11} \delta F_{\sigma,i}^{(2)} + \delta^{\text{WF}} F_\sigma^{(2)} + \delta^{\text{CR}} F_\sigma^{(2)}. \quad (4.63)$$

Various aspects of these results are discussed in detail in Sect. 5.

4.3.1 Analogy with Catani's formula

As we show below, the LL and NLL corrections (4.63) can be written in a form that is analogous to Catani's formula for two-loop mass singularities in massless QCD [26]. In particular, we find that the two-loop corrections can be expressed in terms of the one-loop functions $I(\epsilon, m)$ and $\Delta I(\epsilon, m)$ defined in (3.9)–(3.10). In the massless case ($m = 0$), these functions are related to the factors $\mathbf{I}^{(1)}$ defined in Eq. (13) of Ref. [26]. Actually, for a matrix element involving an external singlet gauge boson and two charged fermions, in the abelian case ($C_F = Q^2$, $C_A = 0$, $T_R = 1$)

$$\frac{\alpha_S(\mu^2)}{2\pi} \mathbf{I}^{(1)}(k\epsilon, \mu^2; \{p\}) \frac{\Gamma(1-k\epsilon)}{\Gamma(1-\epsilon)} e^{(1-k)\gamma_E \epsilon} = \frac{\alpha}{4\pi} N_\epsilon Q^2 I(k\epsilon, 0) \left(\frac{-s}{\mu^2} \right)^{(1-k)\epsilon}, \quad (4.64)$$

at the renormalization scales $\mu = \mu_e = \mu_w$, where the coupling constant of Ref. [26] is related to α by

$$\alpha_S(\mu^2) = \left(\frac{4\pi\mu_0^2}{\mu^2} \right)^\epsilon e^{-\gamma_E \epsilon} \alpha, \quad (4.65)$$

to one-loop accuracy, whereas for the corresponding β -function coefficients we have $4\pi\beta_0 = b_e^{(1)}$. In order to write the two-loop LL and NLL corrections in a compact way, it is useful to define

$$J(\epsilon, m, \mu) := \frac{1}{\epsilon} \left[I(2\epsilon, m) - \left(\frac{-s}{\mu^2} \right)^\epsilon I(\epsilon, m) \right] \quad (4.66)$$

and the corresponding subtracted functions

$$\Delta J(\epsilon, m, \mu) := J(\epsilon, m, \mu) - J(\epsilon, M_W, \mu). \quad (4.67)$$

In the massless abelian case, the function (4.66) is related to the combination of $\mathbf{I}^{(1)}$ functions that corresponds to the two-loop next-to-leading mass singularities proportional to β_0 in Eq. (19) of Ref. [26],

$$\begin{aligned} & \left[\frac{\alpha_S(\mu^2)}{2\pi} \right]^2 \frac{2\pi\beta_0}{\epsilon} \left[\mathbf{I}^{(1)}(2\epsilon, \mu^2; \{p\}) \frac{\Gamma(1-2\epsilon)}{\Gamma(1-\epsilon)} e^{-\gamma_E \epsilon} - \mathbf{I}^{(1)}(\epsilon, \mu^2; \{p\}) \right] = \\ & = \left[\frac{\alpha}{4\pi} N_\epsilon \right]^2 Q^2 b_e^{(1)} J(\epsilon, 0, \mu) \Gamma(1-\epsilon) e^{-\gamma_E \epsilon} \stackrel{\text{NLL}}{=} \left[\frac{\alpha}{4\pi} N_\epsilon \right]^2 Q^2 b_e^{(1)} J(\epsilon, 0, \mu). \end{aligned} \quad (4.68)$$

4.3.2 Results

We find that, at the renormalization scales $\mu_e = \mu_w = M_W$, the two-loop form factors (4.63) can be written in terms of the one-loop form factors (3.8)–(3.10),

$$\begin{aligned} e^2 \delta F_\sigma^{(1)} &\stackrel{\text{NLL}}{=} \left[g_1^2 \left(\frac{Y_\sigma}{2} \right)^2 + g_2^2 C_\sigma \right] I(\epsilon, M_W) \\ &\quad + \left[g_1^2 \left(\frac{Y_\sigma}{2} \right)^2 + g_2^2 (T_\sigma^3)^2 - e^2 Q^2 \right] \Delta I(\epsilon, M_Z) + e^2 Q^2 \Delta I(\epsilon, 0), \end{aligned} \quad (4.69)$$

and the functions (4.66)–(4.67) as

$$\begin{aligned} e^4 \delta F_\sigma^{(2)} \Big|_{\mu_i=M_W} &\stackrel{\text{NLL}}{=} \frac{1}{2} \left[e^2 \delta F_\sigma^{(1)} \right]^2 + e^2 \left[g_1^2 b_1^{(1)} \left(\frac{Y_\sigma}{2} \right)^2 + g_2^2 b_2^{(1)} C_\sigma \right] J(\epsilon, M_W, M_W) \\ &\quad + e^4 b_{\text{QED}}^{(1)} Q^2 \Delta J(\epsilon, 0, M_W). \end{aligned} \quad (4.70)$$

Here, the first term on the right-hand side can be regarded as the result of the exponentiation of the one-loop form factors. This term contains the products of one-loop functions

$$\begin{aligned} [I(\epsilon, M_W)]^2 &\stackrel{\text{NLL}}{=} L^4 - 6L^3 + \mathcal{O}(\epsilon), \\ [\Delta I(\epsilon, M_Z)]^2 &\stackrel{\text{NLL}}{=} 0, \\ [\Delta I(\epsilon, 0)]^2 &\stackrel{\text{NLL}}{=} 4\epsilon^{-4} - 4L^2\epsilon^{-2} - \frac{8}{3}L^3\epsilon^{-1} + 12\epsilon^{-3} + 12L\epsilon^{-2} - 8L^3 + \mathcal{O}(\epsilon), \\ I(\epsilon, M_W) \Delta I(\epsilon, 0) &\stackrel{\text{NLL}}{=} 2L^2\epsilon^{-2} + \frac{4}{3}L^3\epsilon^{-1} - \frac{1}{2}L^4 - 6L\epsilon^{-2} + 7L^3 + \mathcal{O}(\epsilon), \\ I(\epsilon, M_W) \Delta I(\epsilon, M_Z) &\stackrel{\text{NLL}}{=} -2l_Z L^3 + \mathcal{O}(\epsilon), \\ \Delta I(\epsilon, M_Z) \Delta I(\epsilon, 0) &\stackrel{\text{NLL}}{=} -4l_Z \left[L\epsilon^{-2} + L^2\epsilon^{-1} \right] + \mathcal{O}(\epsilon), \end{aligned} \quad (4.71)$$

whereas the functions J and ΔJ , which are associated to the one-loop β -function coefficients, yield the NLL contributions

$$\begin{aligned} J(\epsilon, M_W, M_W) &\stackrel{\text{NLL}}{=} \frac{1}{3}L^3 + \mathcal{O}(\epsilon), \\ \Delta J(\epsilon, 0, M_W) &\stackrel{\text{NLL}}{=} \frac{3}{2}\epsilon^{-3} + 2L\epsilon^{-2} + L^2\epsilon^{-1} + \mathcal{O}(\epsilon). \end{aligned} \quad (4.72)$$

The dependence of the two-loop form factors on the renormalization scales μ_e and μ_w , which originates from the counterterms (4.59)–(4.60), is easily obtained by shifting the couplings in the one-loop form factors. This results into

$$\begin{aligned} e^4 \delta F_\sigma^{(2)} - \left[e^4 \delta F_\sigma^{(2)} \right]_{\mu_i=M_W} &\stackrel{\text{NLL}}{=} \\ &\stackrel{\text{NLL}}{=} e^2 \left[g_1^2 b_1^{(1)} \left(\frac{Y_\sigma}{2} \right)^2 + g_2^2 b_2^{(1)} C_\sigma \right] [J(\epsilon, M_W, \mu_w) - J(\epsilon, M_W, M_W)] \\ &\quad + e^4 b_e^{(1)} Q^2 [\Delta J(\epsilon, 0, \mu_w) - \Delta J(\epsilon, 0, M_W)] \\ &\quad + e^2 b_{\text{QED}}^{(1)} \left\{ \left[g_1^2 \left(\frac{Y_\sigma}{2} \right)^2 + g_2^2 C_\sigma \right] [J(\epsilon, M_W, \mu_e) - J(\epsilon, M_W, \mu_w)] \right. \\ &\quad \left. + e^2 Q^2 [\Delta J(\epsilon, 0, \mu_e) - \Delta J(\epsilon, 0, \mu_w)] \right\}. \end{aligned} \quad (4.73)$$

Within the OS scheme, where $\mu_w = M_W$, (4.73) reduces to the last two lines with

$$\begin{aligned} J(\epsilon, M_W, \mu_e) - J(\epsilon, M_W, M_W) &\stackrel{\text{NLL}}{=} -l_{\mu_e} L^2 + \mathcal{O}(\epsilon), \\ \Delta J(\epsilon, 0, \mu_e) - \Delta J(\epsilon, 0, M_W) &\stackrel{\text{NLL}}{=} -l_{\mu_e} \left[2\epsilon^{-2} + (2L - l_{\mu_e}) \epsilon^{-1} - l_{\mu_e} \left(L - \frac{1}{3} l_{\mu_e} \right) \right] + \mathcal{O}(\epsilon). \end{aligned} \quad (4.74)$$

5 Discussion

In this section, we discuss various features of the results (4.70)–(4.74) and compare them with Refs. [17, 18, 19, 26]. In particular, we focus on the effects originating from various aspects of spontaneous symmetry breaking, such as gauge-boson mixing, mass gaps and couplings with mass dimension. To this end, we first consider various subsets of the EW two-loop corrections corresponding to simpler gauge theories, such as massless QED or an $SU(2) \times U(1)$ theory with gauge-boson masses $M_A = M_Z = M_W$, where these aspects are absent or only partially present.

5.1 Special cases

Our final result, as well as the contributions from individual Feynman diagrams and counterterms in Sects. 3 and 4, and App. B, have been written in such a form that the following special cases can be obtained by simple substitutions.

- (i) We can consider a Higgsless theory by omitting the diagrams 8–10, as well as the scalar contributions to the β -function, i.e.

$$b_{\Phi,1}^{(1)} = b_{\Phi,2}^{(1)} = b_{\Phi,e}^{(1)} = 0. \quad (5.1)$$

- (ii) We can treat the top quark as massless by setting

$$m_t = 0, \quad b_{\text{QED}}^{(1)} = b_{F,e}^{(1)}, \quad (5.2)$$

so that in contrast to (B.6), which corresponds to $m_t \sim M_W$, also the top quark contributes to the QED β -function.

- (iii) As discussed in Sect. 2.4, the mixing effects can be consistently removed by setting

$$Y_\Phi = 0, \quad s_w = 0, \quad c_w = 1, \quad M_Z = M_W. \quad (5.3)$$

In this case, the photon decouples from the weak bosons as well as from the Higgs doublet, since all components of Φ have electric charge $eQ_\Phi = g_1 Y_\Phi / 2 = 0$. As a consequence, the photonic contributions to the diagrams 3 and 6–10 vanish. In particular, the diagrams 7, 8, and 10, which provide NLL contributions only via A–Z mixing-energies, do not contribute at all.

- (iv) After the mixing has been removed, one can restrict oneself to a simple $U(1)$ gauge group with a massless photon by setting

$$g_2 = 0, \quad g_1 = e, \quad Y/2 = Q, \quad b_1^{(1)} = b_e^{(1)}. \quad (5.4)$$

(v) The nonabelian $SU(2) \times U(1)$ interactions can be replaced by abelian $U(1) \times U(1)$ interactions, with a massless photon and a massive Z boson, by setting

$$C_\sigma = (T_\sigma^3)^2, \quad C_A = 0, \quad d_2 = 1, \quad L = \log\left(\frac{-s}{M_Z^2}\right), \quad l_Z = 0. \quad (5.5)$$

As a consequence, the diagrams 3 and 6–8, as well as the gauge-boson and ghost contributions to the β -function, $b_{V,1}^{(1)}$, $b_{V,2}^{(1)}$, and $b_{V,e}^{(1)}$, vanish.

(vi) The effects originating from the gap between the Z - and the W -boson mass in the weak-boson propagators⁹ can be removed by setting

$$M_Z = M_W \quad (5.6)$$

in all diagrams as well as in the WFRCS. This implies $l_Z = 0$. When we study the effects of (5.6) on the diagrammatic calculation we do not use the identity (2.21), which is violated in the case of a non-vanishing mixing angle ($c_W \neq 1$).

(vii) Finally, one can consider the case where one sets the same mass M_W in the propagators of all gauge bosons, A , Z , and W^\pm . As discussed in Sect. 2.5, this is obtained by the substitution

$$Q = 0, \quad (5.7)$$

combined with (5.6). In this case, the diagrams 7, 8, and 10 vanish.

In the following, we apply various combinations of the above substitutions to each individual Feynman diagram and discuss their effect on the resulting two-loop corrections (4.63).

5.1.1 Massless QED

The case of massless QED is obtained by combining the substitutions (i)–(iv). In this case, the one-loop form factors read

$$e^2 \delta F_\sigma^{(1)} \stackrel{\text{NLL}}{=} e^2 Q^2 I(\epsilon, 0), \quad (5.8)$$

and at two loops we obtain

$$e^4 \delta F_\sigma^{(2)} \stackrel{\text{NLL}}{=} \frac{1}{2} e^4 Q^4 [I(\epsilon, 0)]^2 + e^4 Q^2 b_{\text{QED}}^{(1)} J(\epsilon, 0, \mu_e), \quad (5.9)$$

where $b_{\text{QED}}^{(1)} = b_e^{(1)} = b_{F,e}^{(1)}$, and to NLL accuracy

$$\begin{aligned} [I(\epsilon, 0)]^2 &\stackrel{\text{NLL}}{=} 4\epsilon^{-4} + 12\epsilon^{-3}, \\ J(\epsilon, 0, \mu_i) &\stackrel{\text{NLL}}{=} \frac{3}{2}\epsilon^{-3} + 2(L - l_{\mu_i})\epsilon^{-2} + (L - l_{\mu_i})^2\epsilon^{-1} + \frac{1}{3}(L - l_{\mu_i})^3 + \mathcal{O}(\epsilon). \end{aligned} \quad (5.10)$$

By means of (4.64) and (4.68), it is easy to see that the above result agrees with the abelian case of Catani's formula for massless QCD [26].

⁹In order to distinguish the weak-boson masses occurring in the propagators from those occurring in couplings with mass dimension, these latter have been written in terms of \mathbf{v} .

5.1.2 Massive $SU(2) \times U(1)$ theory

Let us consider the case where we suppress the gauge-boson mass gaps by replacing all gauge-boson masses with M_W in the propagators, but keeping all other features of the EW theory unchanged. In this case, which is obtained by the substitutions (vi) and (vii), the one-loop form factors read

$$e^2 \delta F_\sigma^{(1)} \stackrel{\text{NLL}}{=} \left[g_1^2 \left(\frac{Y_\sigma}{2} \right)^2 + g_2^2 C_\sigma \right] I(\epsilon, M_W), \quad (5.11)$$

and at two loops, for $\mu_e = \mu_w = M_W$, we obtain

$$\begin{aligned} e^4 \delta F_\sigma^{(2)} \Big|_{\mu_i=M_W} &\stackrel{\text{NLL}}{=} \frac{1}{2} \left[g_1^2 \left(\frac{Y_\sigma}{2} \right)^2 + g_2^2 C_\sigma \right]^2 [I(\epsilon, M_W)]^2 \\ &+ e^2 \left[g_1^2 b_1^{(1)} \left(\frac{Y_\sigma}{2} \right)^2 + g_2^2 b_2^{(1)} C_\sigma \right] J(\epsilon, M_W, M_W). \end{aligned} \quad (5.12)$$

We note that the two-loop NLL contributions that are proportional to the β -function coefficients in (5.12) can be written, analogously to the massless case (5.9), in terms of the function $J(\epsilon, M_W, M_W)$, which involves a factor ϵ^{-1} in its definition (4.66). This indicates that the two-loop NLL's of the type $b_i^{(1)} L^3$ are related to the one-loop LL's of order ϵL^3 in $I(\epsilon, M_W)$.

We also note that the above result is independent of the gauge-boson mixing as well as of the symmetry-breaking mechanism. In fact, if we compute all diagrams in the unmixed case (iii), if we completely remove the Higgs doublet with the substitutions (i), or if we simply neglect symmetry breaking ($\mathbf{v} = 0$), the resulting two-loop form factors remain unchanged. In particular, in absence of the mass gaps between the gauge bosons, each of the diagrams 1–11 is independent of the weak mixing angle. Moreover, the only diagram that is proportional to the vev, i.e. diagram 8, does not contribute.

Using (4.71)–(4.72) we see that, in the special cases of pure $SU(2)$ and pure $U(1)$ massive theories, which result from $g_1 = 0$ and $g_2 = 0$, respectively, the result (5.12) is in agreement with Ref. [18].

5.1.3 Massless $U(1)$ theory with heavy top quark and scalar doublet

In order to discuss the effect resulting from the gap between the (vanishing) mass of the photon and the heavy masses of the top quark and scalar particles, let us consider the case of a $U(1)$ theory with fermions and a scalar doublet, which is obtained by removing symmetry breaking ($\mathbf{v} = 0$) and combining the substitutions¹⁰ (iii) and (iv). In this case, the one-loop form factors are as in (5.8) and at two loops, for $\mu_e = \mu_w = M_W$, we obtain

$$e^4 \delta F_\sigma^{(2)} \Big|_{\mu_i=M_W} \stackrel{\text{NLL}}{=} \frac{1}{2} e^4 Q^4 [I(\epsilon, 0)]^2 + e^4 Q^2 \left[b_e^{(1)} J(\epsilon, M_W, M_W) + b_{\text{QED}}^{(1)} \Delta J(\epsilon, 0, M_W) \right]. \quad (5.13)$$

¹⁰In this case, we do not use (2.22) and keep $Y_\Phi \neq 0$ in (iii), so that the components of the scalar doublet have a non-vanishing electric charge, $eQ_\Phi = g_1 Y_\Phi / 2$.

As one can easily see by using the definition (4.67), the only difference between (5.13) and the result (5.9) for massless QED consists of NLL's proportional to $(b_e^{(1)} - b_{\text{QED}}^{(1)})$ times $J(\epsilon, M_W, M_W)$. Such terms, which result from diagrams 9 and 10, from the top-quark contribution to diagram 11, and from the corresponding heavy-particle contributions to the β -function, do not give rise to infrared $1/\epsilon$ poles and behave as if the photon would be heavy [see (5.12)].

5.1.4 Mass-gap effects within an abelian $U(1) \times U(1)$ theory

In order to discuss the effects resulting from the gap between the vanishing mass of the photon ($\lambda = 0$) and the weak-boson mass scale M_W , let us consider a $U(1) \times U(1)$ theory with a massless photon and a Z boson with mass¹¹ $M_Z = M_W$ coupled to (massless and heavy) fermions and to the Higgs doublet. In this case, which results from the substitutions (v), the one-loop form factors read

$$e^2 \delta F_\sigma^{(1)} \stackrel{\text{NLL}}{=} \left[g_1^2 \left(\frac{Y_\sigma}{2} \right)^2 + g_2^2 (T_\sigma^3)^2 \right] I(\epsilon, M_W) + e^2 Q^2 \Delta I(\epsilon, 0), \quad (5.14)$$

and at two loops, for $\mu_e = \mu_w = M_W$, we obtain

$$\begin{aligned} e^4 \delta F_\sigma^{(2)} \Big|_{\mu_i=M_W} &\stackrel{\text{NLL}}{=} \frac{1}{2} \left\{ \left[g_1^2 \left(\frac{Y_\sigma}{2} \right)^2 + g_2^2 (T_\sigma^3)^2 \right] I(\epsilon, M_W) + e^2 Q^2 \Delta I(\epsilon, 0) \right\}^2 \\ &+ e^2 \left[g_1^2 b_1^{(1)} \left(\frac{Y_\sigma}{2} \right)^2 + g_2^2 b_2^{(1)} (T_\sigma^3)^2 \right] J(\epsilon, M_W, M_W) \\ &+ e^4 b_{\text{QED}}^{(1)} Q^2 \Delta J(\epsilon, 0, M_W). \end{aligned} \quad (5.15)$$

The various products of one-loop functions that appear in this expression for the two-loop corrections have been expanded in (4.71) and (4.72), including terms up to the order ϵ^0 . It is interesting to observe that certain one-loop functions on the right-hand side of (5.15) need to be expanded beyond order ϵ^0 in order to reproduce all divergent and finite parts of the result (4.63) of the diagrammatic NLL calculation. Indeed, in the products of the type $I(\epsilon, M_W) \Delta I(\epsilon, 0)$, i.e. combinations of massive and massless one-loop contributions, the massive one-loop terms have to be expanded up to the order ϵ^2 , since the massless one-loop terms involve poles of order ϵ^{-2} . This means, for instance, that the two-loop corrections of order L^4 in (5.15) receive contributions from the one-loop corrections of order $\epsilon^2 L^4$.

As in Sect. 5.1.2, also in the $U(1) \times U(1)$ case we find that the final result does not change if one performs the diagrammatic calculation by neglecting the gauge-boson mixing and/or the symmetry-breaking mechanism. In particular, the diagram 8 does not contribute in the abelian case.

A detailed comparison of the result (5.15) with Refs. [17, 18, 19] is not possible, since we have regulated mass singularities dimensionally and we did not include real electromagnetic corrections. However, we observe that (5.15), and in particular its dependence

¹¹Despite of the fact that there are no W bosons in the abelian case, here we assume $M_Z = M_W$ since we have chosen M_W as scale of the logarithms (2.10) originating from massive gauge bosons.

on the gauge-boson mass gap, $\lambda \ll M_W$, confirms the approach that has been adopted in Refs. [17, 18, 19] to resum the EW corrections. Indeed, we see that the only difference between (5.15) and the corresponding result for $\lambda = M_W$, i.e. the abelian case of (5.12), consists of terms proportional to $Q^2 \Delta I(\epsilon, 0)$ and $Q^2 b_{\text{QED}}^{(1)} \Delta J(\epsilon, 0, M_W)$, which correspond to QED corrections (with $\lambda = 0$) subtracted at the scale $\lambda = M_W$. This means that the two-loop corrections in presence of a mass gap $\lambda \ll M_W$ result from the corrections within an unbroken and unmixed gauge theory with $\lambda = M_W$ with additional mass-gap effects that are of pure electromagnetic nature.

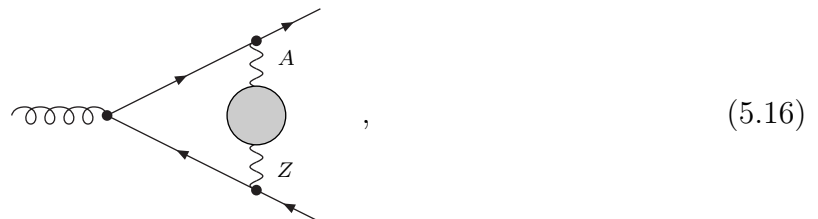
5.1.5 Mixing, Z–W mass gap and symmetry breaking within the electroweak theory

Finally, let us discuss the results (4.70)–(4.74), which are obtained by considering all two-loop diagrams within the spontaneously broken EW theory. We first observe that the only two-loop contributions depending on the gaps between the heavy-particle masses (2.13) are the NLL's proportional to $l_Z = \log(M_Z/M_W)$ that arise from the squared one-loop corrections in (4.70) via the $\Delta I(\epsilon, M_Z)$ subtracted terms in (4.69). This means that such Z–W mass-gap contributions exponentiate.

If we neglect these NLL's proportional to l_Z , the result (4.70) is analogous to (5.15) and confirms the approach adopted in Refs. [17, 18, 19] to resum the EW corrections, as discussed in Sect. 5.1.4 for the abelian case. In particular, the effects resulting from the gap between the (vanishing) photon mass and the weak-boson mass scale turn out to be of QED nature also in the non-abelian case.

We note that, apart from the l_Z contributions, the result (4.70) seem to be insensitive to the gauge-boson mixing, the Z–W mass gap, and the symmetry breaking. Indeed, if we compute all diagrams in absence of mixing, with $M_W = M_Z$ in the weak-boson propagators, and $\mathbf{v} = 0$, we obtain the same two-loop form factors (4.70) with $l_Z = 0$. However, when we perform the calculation within the mixed spontaneously broken EW theory, we observe that the mixing effects drop out as a result of subtle cancellations between different diagrams, which take place only if the Z–W mass gap and the vev are properly taken into account.

In order to understand these mixing cancellations, let us consider the behaviour of the diagrams involving A–Z mixing-energies, i.e. diagrams of the type



which we call A–Z mixing diagrams. The combination of all A–Z mixing diagrams 6–11 yields the infrared-divergent contribution¹²,

$$\Delta\delta F_{\sigma,AZ}^{(2)} \stackrel{\text{NLL}}{=} 4e^2 g_2^2 s_W c_W Q I_\sigma^Z K(M_W, M_Z, \mathbf{v}) \left[\epsilon^{-3} + L \epsilon^{-2} - \frac{2}{3} L^3 \right], \quad (5.17)$$

¹²Here we consider the infrared-divergent Δ -contributions corresponding to the subtracted terms in (2.30).

where

$$\begin{aligned} K(M_W, M_Z, \mathbf{v}) &= \left(\frac{M_W}{M_Z}\right)^2 [4C_A - 3(d_2 - 1)] + \left(\frac{g_2 \mathbf{v}}{2c_W M_Z}\right)^2 [C_A - (d_2 - 1)c_W^2] \\ &= 2 \left\{ \left(\frac{M_W}{M_Z}\right)^2 + s_W^2 \left(\frac{g_2 \mathbf{v}}{2c_W M_Z}\right)^2 \right\}. \end{aligned} \quad (5.18)$$

We note that only the bosonic diagrams 6–8 contribute to (5.17), whereas the fermionic A–Z mixing diagrams 11, and the combination of scalar A–Z mixing diagrams 9 and 10 are irrelevant. The A–Z mixing contributions (5.17) arise only in presence of mixing ($s_W \neq 0$) and are of non-abelian nature, since the coefficient (5.18) vanishes within an abelian $U(1) \times U(1)$ theory, where $C_A = 0$ and $d_2 = 1$. Moreover, they involve the only (NLL) contribution that depends on the vev, i.e. diagram 8.

We see that, in contrast to the contributions from all other diagrams, (5.17)–(5.18) depend linearly on the ratios $(M_W/M_Z)^2$ or $(\mathbf{v}/M_Z)^2$. For instance, the A–Z mixing diagrams yield infrared-divergent terms proportional to $(M_W/M_Z)^2 \epsilon^{-3}$ that arise as combinations of UV singularities proportional to $M_W^2 \epsilon^{-1}$ from tadpole mixing-energy subdiagrams, together with soft-collinear singularities proportional to $M_Z^{-2} \epsilon^{-2}$ from the region where the photon momentum vanishes and the Z-boson propagator equals $-ig^{\mu\nu}/M_Z^2$.

In the final result, we find that the A–Z mixing contribution (5.17) cancels against a corresponding mixing contribution proportional to $s_W Q I_\sigma^Z [\epsilon^{-3} + L \epsilon^{-2} - 2/3 L^3]$ from all other diagrams¹³. In order to ensure this mixing cancellation, it is crucial to take into account the relations (2.20) between the weak-boson masses and the vev. In particular, one has to compute the A–Z mixing diagrams using $M_W = c_W M_Z$, i.e. different masses in the weak-boson propagators.

If one would neglect the vev, i.e. diagram 8, or if one would compute all diagrams with $M_W = M_Z$, the mixing cancellations would be destroyed, and one would find deviations of order ϵ^{-3} with respect to (4.70). However, it is interesting to note that if one simultaneously omits the diagram 8 ($\mathbf{v} = 0$) and one uses $M_W = M_Z$ in the propagators, then (5.18) remains unchanged, i.e. the mixing cancellations are preserved and one obtains the same result as in (4.70). This means that the diagram 8 cancels the Z–W mass-gap effects resulting from the gauge-boson- and ghost- A–Z mixing diagrams 6 and 7.

6 Conclusions

We have considered the one- and two-loop virtual electroweak (EW) corrections to the form factors for an $SU(2) \times U(1)$ singlet gauge boson of invariant mass s coupling to massless chiral fermions. In the asymptotic region $s \gg M_W^2$, we have computed mass singularities in $D = 4 - 2\epsilon$ dimensions taking into account leading logarithms (LL's) and next-to-leading logarithms (NLL's). This approximation includes combinations $\alpha^l \epsilon^k \log^{j+k}(s/M_W^2)$ of mass-singular logarithms and $1/\epsilon$ poles, with $j = 2l, 2l - 1$, and $-j \leq k \leq 4 - 2l$. The heavy particle masses, $M_Z \sim M_W \sim m_t \sim M_H$, have been assumed to be of the same order but not equal.

We found that the EW two-loop LL's and NLL's result from the exponentiation of the corresponding one-loop contributions plus additional NLL's that are proportional to the

¹³Such contribution corresponds to (5.17) with the factor (5.18) replaced by -2 .

one-loop β -function coefficients. This result has been expressed in a form that corresponds to a generalization of Catani's two-loop formula for massless QCD.

If one neglects the NLL's proportional to $\log(M_Z/M_W)$, which turn out to exponentiate, the result confirms the approach that has been adopted in Refs. [17, 18, 19] to resum the EW corrections. Indeed, the two-loop EW LL's and NLL's can be expressed through the corresponding corrections within an unbroken and unmixed $SU(2) \times U(1)$ theory where all EW gauge bosons have mass M_W and additional effects resulting from the gap between the vanishing photon mass, $\lambda = 0$, and the weak-boson mass scale M_W . Such photonic mass-gap effects turn out to consist of pure QED corrections, with $\lambda = 0$, subtracted at the scale $\lambda = M_W$.

Apart from the $\log(M_Z/M_W)$ -contributions, the effects from the gauge-boson mixing, the Z-W mass gap, and the symmetry breaking cancel in the final result. However, we found that this simple behaviour of the two-loop form factors is ensured by subtle cancellations between subleading mass singularities from different diagrams where, in contrast to the assumptions (i)–(iii) discussed in Sect. 1, the details of spontaneous symmetry breaking cannot be neglected. In particular, we have stressed that

- (i) Couplings with mass dimension, i.e. proportional to the vacuum expectation value v , cannot be neglected in the massless limit $M_W^2/s \rightarrow 0$.
- (ii) Diagrams involving A-Z mixing-energies, which give rise to contributions proportional to $(M_W/M_Z)^2$ and $(v/M_Z)^2$, have to be computed using different masses, $M_W \neq M_Z$, in the weak-boson propagators.
- (iii) The mixing effects drop out as a result of cancellations that take place only if the relations between the weak-boson masses, the weak mixing angle and the vacuum expectation value are properly taken into account.

We note that the symmetry-breaking effects were restricted to a small subset of diagrams in this form-factor calculation, since the Higgs sector is coupled to the massless fermions only via one-loop insertions in the gauge-boson self-energies and mixing-energies. Therefore, it would be interesting to extend the study of two-loop subleading mass singularities to processes involving heavy external particles, which are directly coupled to the Higgs sector.

Acknowledgments

I would like to thank A. Denner, J. H. Kühn and O. Veretin for fruitful discussions. I am grateful to A. Denner for carefully reading the manuscript.

A Loop integrals

In this appendix, we list the explicit expressions for the Feynman integrals that contribute to the one- and two-loop diagrams discussed in Sects. 3 and 4. In order to keep our expressions as compact as possible we define the momenta

$$\begin{aligned} k_1 &= l_1 + p_1, & k_2 &= l_2 + p_1, & k_3 &= l_1 + l_2 + p_1, \\ q_1 &= l_1 - p_2, & q_2 &= l_2 - p_2, & q_3 &= l_1 + l_2 - p_2, & l_3 &= -l_1 - l_2, \end{aligned} \quad (\text{A.1})$$

for massive and massless propagators we use the notation

$$P(q, m) := q^2 - m^2 + i0, \quad P(q) := q^2 + i0, \quad (\text{A.2})$$

and for triple gauge-boson couplings we write

$$\Gamma^{\mu_1 \mu_2 \mu_3}(l_1, l_2, l_3) := g^{\mu_1 \mu_2}(l_1 - l_2)^{\mu_3} + g^{\mu_2 \mu_3}(l_2 - l_3)^{\mu_1} + g^{\mu_3 \mu_1}(l_3 - l_1)^{\mu_2}. \quad (\text{A.3})$$

The normalization factors occurring in (2.6) and (2.7) are absorbed into the integration measure

$$d\tilde{l}_i := \frac{(4\pi)^2}{N_\epsilon} \mu_0^{4-D} \frac{d^D l_i}{(2\pi)^D} = \frac{1}{\pi^2} \Gamma\left(\frac{D}{2} - 1\right) (-s\pi)^{2-D/2} d^D l_i, \quad (\text{A.4})$$

and for the projection introduced in (2.4) we use the shorthand

$$\text{Pr}(\Gamma^\nu) := \frac{1}{2(2-D)s} \text{Tr}(\gamma_\nu \not{p}_1 \Gamma^\nu \not{p}_2). \quad (\text{A.5})$$

With this notation we have

$$\begin{aligned} D_0(m_1) &:= -i \int d\tilde{l}_1 \frac{\text{Pr}(\gamma^{\mu_1} \not{k}_1 \gamma^\nu \not{q}_1 \gamma_{\mu_1})}{P(l_1, m_1) P(k_1) P(q_1)}, \\ D_1(m_1, m_2) &:= - \int d\tilde{l}_1 d\tilde{l}_2 \frac{\text{Pr}(\gamma^{\mu_1} \not{k}_1 \gamma^{\mu_2} \not{k}_3 \gamma^\nu \not{q}_3 \gamma_{\mu_2} \not{q}_1 \gamma_{\mu_1})}{P(l_1, m_1) P(l_2, m_2) P(k_1) P(k_3) P(q_1) P(q_3)}, \\ D_2(m_1, m_2) &:= - \int d\tilde{l}_1 d\tilde{l}_2 \frac{\text{Pr}(\gamma^{\mu_1} \not{k}_1 \gamma^{\mu_2} \not{k}_3 \gamma^\nu \not{q}_3 \gamma_{\mu_1} \not{q}_2 \gamma_{\mu_2})}{P(l_1, m_1) P(l_2, m_2) P(k_1) P(k_3) P(q_2) P(q_3)}, \\ D_3(m_1, m_2, m_3) &:= \int d\tilde{l}_1 d\tilde{l}_2 \frac{\text{Pr}(\gamma^{\mu_1} \not{k}_1 \gamma^{\mu_2} \not{k}_3 \gamma^\nu \not{q}_3 \gamma^{\mu_3}) \Gamma_{\mu_1 \mu_2 \mu_3}(l_1, l_2, l_3)}{P(l_1, m_1) P(l_2, m_2) P(l_3, m_3) P(k_1) P(k_3) P(q_3)}, \\ D_4(m_1, m_2) &:= - \int d\tilde{l}_1 d\tilde{l}_2 \frac{\text{Pr}(\gamma^{\mu_1} \not{k}_1 \gamma^{\mu_2} \not{k}_3 \gamma_{\mu_2} \not{k}_1 \gamma^\nu \not{q}_1 \gamma_{\mu_1})}{P(l_1, m_1) P(l_2, m_2) [P(k_1)]^2 P(k_3) P(q_1)}, \\ D_5(m_1, m_2) &:= - \int d\tilde{l}_1 d\tilde{l}_2 \frac{\text{Pr}(\gamma^{\mu_2} \not{k}_2 \gamma^{\mu_1} \not{k}_3 \gamma_{\mu_2} \not{k}_1 \gamma^\nu \not{q}_1 \gamma_{\mu_1})}{P(l_1, m_1) P(l_2, m_2) P(k_1) P(k_3) P(k_2) P(q_1)}, \\ D_6(m_1, m_2, m_3, m_4) &:= \int d\tilde{l}_1 d\tilde{l}_2 \frac{\text{Pr}(\gamma^{\mu_1} \not{k}_1 \gamma^\nu \not{q}_1 \gamma_{\mu_4})}{P(l_1, m_1) P(l_2, m_2) P(l_3, m_3) P(l_1, m_4) P(k_1) P(q_1)} \times \\ &\quad \times [\Gamma_{\mu_1 \mu_2 \mu_3}(l_1, l_2, l_3) \Gamma^{\mu_4 \mu_2 \mu_3}(l_1, l_2, l_3) + 2l_{2\mu_1} l_3^{\mu_4}], \\ D_7(m_1, m_2, m_3) &:= \int d\tilde{l}_1 d\tilde{l}_2 \frac{\text{Pr}(\gamma^{\mu_1} \not{k}_1 \gamma^\nu \not{q}_1 \gamma_{\mu_1})}{P(l_1, m_1) P(l_2, m_2) P(l_1, m_3) P(k_1) P(q_1)}, \\ D_8(m_1, m_2, m_3, m_4) &:= \int d\tilde{l}_1 d\tilde{l}_2 \frac{\text{Pr}(\gamma^{\mu_1} \not{k}_1 \gamma^\nu \not{q}_1 \gamma_{\mu_1})}{P(l_1, m_1) P(l_2, m_2) P(l_3, m_3) P(l_1, m_4) P(k_1) P(q_1)}, \\ D_9(m_1, m_2, m_3, m_4) &:= - \int d\tilde{l}_1 d\tilde{l}_2 \frac{\text{Pr}(\gamma^{\mu_1} \not{k}_1 \gamma^\nu \not{q}_1 \gamma_{\mu_4}) (l_2 - l_3)_{\mu_1} (l_2 - l_3)^{\mu_4}}{P(l_1, m_1) P(l_2, m_2) P(l_3, m_3) P(l_1, m_4) P(k_1) P(q_1)}, \\ D_{10}(m_1, m_2, m_3) &:= D_7(m_1, m_2, m_3), \\ D_{11,0}(m_1, m_2, m_3, m_4) &:= - \int d\tilde{l}_1 d\tilde{l}_2 \frac{\text{Pr}(\gamma^{\mu_1} \not{k}_1 \gamma^\nu \not{q}_1 \gamma_{\mu_4}) \text{Tr}(\gamma_{\mu_1} \not{l}_2 \gamma^{\mu_4} \not{l}_3)}{P(l_1, m_1) P(l_2, m_2) P(l_3, m_3) P(l_1, m_4) P(k_1) P(q_1)}, \\ D_{11,m}(m_1, m_2, m_3, m_4) &:= -4D_8(m_1, m_2, m_3, m_4). \end{aligned} \quad (\text{A.6})$$

In order to isolate the effects originating from the mass gaps as discussed in Sect. 2.5, we introduce the subtracted loop integrals

$$\Delta D_k(m_1, \dots, m_n) := D_k(m_1, \dots, m_n) - [D_k(m_1, \dots, m_n)]_{m_i=M_W}. \quad (\text{A.7})$$

B β -function coefficients

In this appendix we give relations and explicit expressions for the one-loop β -function coefficients $b_1^{(1)}$, $b_2^{(1)}$, $b_e^{(1)}$, and $b_{\text{QED}}^{(1)}$, which have been used in the calculation. For more details we refer to Ref. [13].

The coefficients $b_1^{(1)}$, $b_2^{(1)}$ and $b_e^{(1)}$, are related to the matrix

$$b_{ab}^{(1)} = b_1^{(1)} \delta_{ab}^{\text{U}(1)} + b_2^{(1)} \delta_{ab}^{\text{SU}(2)}, \quad a, b = A, Z, \pm, \quad (\text{B.1})$$

which corresponds to the residues of ultraviolet poles of the gauge-boson self-energies and mixing-energies. Here, $\delta^{\text{U}(1)}$ and $\delta^{\text{SU}(2)}$ are the projectors defined in (2.27). The coefficient corresponding to the electric-charge renormalization is given by

$$b_e^{(1)} = b_{AA}^{(1)} = c_w^2 b_1^{(1)} + s_w^2 b_2^{(1)}. \quad (\text{B.2})$$

Each β -function coefficient $b_k^{(1)} = b_1^{(1)}, b_2^{(1)}, b_e^{(1)}, b_{ab}^{(1)}$ receives contributions from the gauge (V), scalar (Φ), and fermionic (F) sectors, and the fermionic contributions result from the sum over $N_G = 3$ generations of leptons (L) and quarks (Q), with $N_c = 3$ colours:

$$b_k^{(1)} = \sum_{R=V,\Phi,F} b_{R,k}^{(1)}, \quad b_{F,k}^{(1)} = N_G \left[b_{L,k}^{(1)} + N_c b_{Q,k}^{(1)} \right]. \quad (\text{B.3})$$

The individual contributions to $b_{ab}^{(1)}$ read¹⁴

$$\begin{aligned} e^2 b_{V,ab}^{(1)} &= \frac{11}{3} e^2 \text{Tr}_V (I^{\bar{a}} I^b) = \frac{11}{3} g_2^2 C_A \delta_{ab}^{\text{SU}(2)}, \\ e^2 b_{\Phi,ab}^{(1)} &= -\frac{1}{3} e^2 \text{Tr}_{\Phi} (I^{\bar{a}} I^b) = -\frac{1}{6} \left[g_1^2 Y_{\Phi}^2 \delta_{ab}^{\text{U}(1)} + g_2^2 \delta_{ab}^{\text{SU}(2)} \right], \\ e^2 b_{\Psi,ab}^{(1)} &= -\frac{2}{3} e^2 \sum_{\rho=\pm} \text{Tr}_{\Psi} (I_{\rho}^{\bar{a}} I_{\rho}^b) = -\frac{2}{3} \left[g_1^2 \sum_{\rho=\pm} \frac{(Y_{\rho})_d^2 + (Y_{\rho})_u^2}{4} \delta_{ab}^{\text{U}(1)} + \frac{1}{2} g_2^2 \delta_{ab}^{\text{SU}(2)} \right], \end{aligned} \quad (\text{B.4})$$

¹⁴Each contribution $b_{R,ab}^{(1)}$ is expressed in terms of the trace

$$e^2 \text{Tr}_R (I^{\bar{a}} I^b) = e^2 \sum_{\varphi_i, \varphi_j \in R} I_{\varphi_i \varphi_j}^{\bar{a}} I_{\varphi_j \varphi_i}^b = \frac{1}{4} g_1^2 \text{Tr}_R (Y^2) \delta_{ab}^{\text{U}(1)} + g_2^2 T_R \delta_{ab}^{\text{SU}(2)},$$

in the corresponding representation $R = V, \Phi, \Psi$. For singlet-, doublet- and triplet-SU(2) representations we have $\text{Tr}_R = 0, 1/2$ and 2, respectively. For $R = \Phi$, since we parametrize the Higgs doublet in terms of its four physical components, we have

$$\text{Tr}_{\Phi} (I^{\bar{a}} I^b) = \frac{1}{2} \sum_{\Phi_i, \Phi_j = H, \chi, \phi^{\pm}} I_{\Phi_i \Phi_j}^{\bar{a}} I_{\Phi_j \Phi_i}^b.$$

where the last line corresponds to a doublet of leptons or quarks ($\Psi = L, Q$) with up- and down- components $\Psi_i = u, d$. The resulting contributions to (B.2) read

$$\begin{aligned} e^2 b_{V,e}^{(1)} &= \frac{11}{3} e^2 \text{Tr}_V (I^A I^A) = \frac{11}{3} g_2^2 s_w^2 C_A, \\ e^2 b_{\Phi,e}^{(1)} &= -\frac{1}{3} e^2 \text{Tr}_\Phi (I^A I^A) = -\frac{1}{6} [g_1^2 c_w^2 Y_\Phi^2 + g_2^2 s_w^2], \\ b_{\Psi,e}^{(1)} &= -\frac{4}{3} \text{Tr}_\Psi (I^A I^A) = -\frac{4}{3} \sum_{\Psi_i=u,d} Q_{\Psi_i}^2. \end{aligned} \quad (\text{B.5})$$

The QED β -function coefficient is given by the light-fermion contributions only, i.e.

$$b_{\text{QED}}^{(1)} = b_{F,e}^{(1)} + \frac{4}{3} N_c Q_t^2. \quad (\text{B.6})$$

References

- [1] S. Haywood, P. R. Hobson, W. Hollik, Z. Kunszt et al., hep-ph/0003275, in *Standard Model Physics (and more) at the LHC*, eds. G. Altarelli and M. L. Mangano, (CERN-2000-004, Genève, 2000) p. 117.
- [2] J. A. Aguilar-Saavedra *et al.*, TESLA Technical Design Report Part III: Physics at an e^+e^- Linear Collider, hep-ph/0106315.
- [3] T. Abe *et al.* [American Linear Collider Working Group Collaboration], in *Proc. of the APS/DPF/DPB Summer Study on the Future of Particle Physics (Snowmass 2001)*, ed. R. Davidson and C. Quigg, SLAC-R-570, *Resource book for Snowmass 2001* [hep-ex/0106055, hep-ex/0106056, hep-ex/0106057, hep-ex/0106058].
- [4] K. Abe *et al.* [ACFA Linear Collider Working Group Collaboration], ACFA Linear Collider Working Group report [hep-ph/0109166].
- [5] M. Kuroda, G. Moultaka and D. Schildknecht, *Nucl. Phys. B* **350** (1991) 25; G. Degrassi and A. Sirlin, *Phys. Rev. D* **46** (1992) 3104; A. Denner, S. Dittmaier and R. Schuster, *Nucl. Phys. B* **452** (1995) 80; A. Denner, S. Dittmaier and T. Hahn, *Phys. Rev. D* **56** (1997) 117; A. Denner and T. Hahn, *Nucl. Phys. B* **525** (1998) 27; M. Beccaria *et al.*, *Phys. Rev. D* **58** (1998) 093014 [hep-ph/9805250].
- [6] V. V. Sudakov, *Sov. Phys. JETP* **3** (1956) 65 [*Zh. Eksp. Teor. Fiz.* **30** (1956) 87].
- [7] M. Ciafaloni, P. Ciafaloni and D. Comelli, *Phys. Rev. Lett.* **84** (2000) 4810 [hep-ph/0001142]; *Nucl. Phys. B* **589** (2000) 359 [hep-ph/0004071]; *Phys. Lett. B* **501** (2001) 216 [hep-ph/0007096]; *Phys. Rev. Lett.* **87** (2001) 211802 [hep-ph/0103315]; *Nucl. Phys. B* **613** (2001) 382 [hep-ph/0103316].
- [8] W. Beenakker *et al.*, *Nucl. Phys. B* **410** (1993) 245; *Phys. Lett. B* **317** (1993) 622.
- [9] P. Ciafaloni and D. Comelli, *Phys. Lett. B* **446** (1999) 278 [hep-ph/9809321].

- [10] M. Beccaria *et al.*, *Phys. Rev. D* **61** (2000) 073005 [hep-ph/9906319]; *Phys. Rev. D* **61** (2000) 011301 [hep-ph/9907389];
M. Beccaria, F. M. Renard and C. Verzegnassi, *Phys. Rev. D* **63** (2001) 053013 [hep-ph/0010205]; *Phys. Rev. D* **64** (2001) 073008 [hep-ph/0103335];
- [11] J. Layssac and F. M. Renard, *Phys. Rev. D* **64** (2001) 053018 [hep-ph/0104205];
G. J. Gounaris, J. Layssac and F. M. Renard, *Phys. Rev. D* **67** (2003) 013012 [hep-ph/0211327].
- [12] A. Denner and S. Pozzorini, *Eur. Phys. J. C* **18** (2001) 461 [hep-ph/0010201]; *Eur. Phys. J. C* **21** (2001) 63 [hep-ph/0104127].
- [13] S. Pozzorini, *doctoral thesis, Universität Zürich, 2001*, hep-ph/0201077.
- [14] E. Accomando, A. Denner and S. Pozzorini, *Phys. Rev. D* **65** (2002) 073003 [hep-ph/0110114].
- [15] U. Aglietti and R. Bonciani, *Nucl. Phys. B* **668** (2003) 3 [hep-ph/0304028].
- [16] G. Passarino, *Nucl. Phys. B* **619** (2001) 257 [hep-ph/0108252];
A. Ferroglia, M. Passera, G. Passarino and S. Uccirati, hep-ph/0311186.
- [17] V. S. Fadin *et al.*, *Phys. Rev. D* **61** (2000) 094002 [hep-ph/9910338].
- [18] J. H. Kühn, A. A. Penin and V. A. Smirnov, *Eur. Phys. J. C* **17** (2000) 97 [hep-ph/9912503];
J. H. Kühn *et al.*, *Nucl. Phys. B* **616** (2001) 286 [hep-ph/0106298].
- [19] M. Melles, *Phys. Rev. D* **63** (2001) 034003 [hep-ph/0004056]; *Phys. Rev. D* **64** (2001) 014011 [hep-ph/0012157]; *Phys. Rev. D* **64** (2001) 054003 [hep-ph/0102097]; *Phys. Rept.* **375** (2003) 219 [hep-ph/0104232].
- [20] M. Melles, *Eur. Phys. J. C* **24** (2002) 193 [hep-ph/0108221].
- [21] M. Melles, *Phys. Lett. B* **495** (2000) 81 [hep-ph/0006077].
- [22] M. Hori, H. Kawamura and J. Kodaira, *Phys. Lett. B* **491** (2000) 275 [hep-ph/0007329].
- [23] W. Beenakker and A. Werthenbach, *Phys. Lett. B* **489** (2000) 148 [hep-ph/0005316];
Nucl. Phys. B **630** (2002) 3 [hep-ph/0112030].
- [24] A. Denner, M. Melles and S. Pozzorini, *Nucl. Phys. B* **662** (2003) 299 [hep-ph/0301241].
- [25] B. Feucht, J. H. Kühn and S. Moch, *Phys. Lett. B* **561** (2003) 111 [hep-ph/0303016].
- [26] S. Catani, *Phys. Lett. B* **427** (1998) 161 [hep-ph/9802439].
- [27] K. Hepp, *Commun. Math. Phys.* **2** (1966) 301.

- [28] M. Roth and A. Denner, *Nucl. Phys. B* **479** (1996) 495 [hep-ph/9605420].
- [29] T. Binoth and G. Heinrich, *Nucl. Phys. B* **585** (2000) 741 [hep-ph/0004013].
- [30] A. Denner, M. Melles and S. Pozzorini, *Nucl. Phys. Proc. Suppl.* **116** (2003) 18 [hep-ph/0211196].
- [31] A. Denner and S. Pozzorini, in preparation.
- [32] A. Denner, *Fortsch. Phys.* **41** (1993) 307.